Aerosolized Hydrogen Peroxide Decontamination of N95 Respirators, with Fit-Testing and Virologic Confirmation of Suitability for Re-Use During the COVID-19 Pandemic

T. Hans Derr[1]*^, Melissa A. James[2]^, Chad V. Kuny[4,8]^, Devanshi Patel[6,8], Prem P. Kandel[5], Cassandra Field[6,8], Matthew D. Beckman[7], Kevin L. Hockett[5,8], Mark A. Bates[3], Troy C. Sutton[6,8], Moriah Szpara[4,8]*

^co-first-authors

[1] Environmental Health and Safety; [2] Animal Resource Program, [3] Occupational Medicine Program, and [4] Departments of Biology, Biochemistry and Molecular Biology, [5] Plant Pathology and Environmental Microbiology, [6] Veterinary and Biomedical Sciences, [7] Statistics, [8] Center for Infectious Disease Dynamics, and the Huck Institutes of the Life Sciences, Pennsylvania State University, University Park, Pennsylvania 16802, USA

*Co-Corresponding Authors

Moriah L. Szpara, PhD
Depts. of Biology, and Biochemistry & Molecular Biology
The Huck Institutes of the Life Sciences
Pennsylvania State University
W-208 Millennium Science Complex (MSC)
University Park, PA 16802 USA
Phone: 814-867-0008
Email: moriah@psu.edu

T. Hans Derr, CIH
Manager, Health & Environmental Programs
Environmental Health & Safety
Pennsylvania State University
6B Eisenhower Deck
University Park, PA 16802
Phone: 814-863-3834
Email: thd12@psu.edu

Author emails:

Mark A. Bates: mxb20@psu.edu
Matthew D. Beckman: mdb268@psu.edu
T. Hans Derr: thd12@psu.edu
Cassandra Field: cif5202@psu.edu
Kevin L. Hockett: klh450@psu.edu
Melissa A. James: maj22@psu.edu
Prem Kandel: puk155@psu.edu
Chad V. Kuny: cvk108@psu.edu
Devanshi Patel: drp5323@psu.edu
Troy C. Sutton: tcs38@psu.edu
Moriah L. Szpara: moriah@psu.edu

Abstract

In response to the current demand for N95 respirators by healthcare workers responding to the COVID-19 pandemic, we evaluated decontamination of N95 respirators using a low concentration aerosolized hydrogen peroxide (aHP) system. This system dispenses a consistent atomized spray of micron-sized, low concentration, hydrogen peroxide (H_2O_2) particles over a treatment cycle. Multiple N95 respirator models were subjected to ten or more cycles of respirator decontamination, and masks were periodically assessed for qualitative and quantitative fit testing to verify respirator integrity. In parallel, we assessed the ability of aHP treatment to inactivate multiple viruses absorbed onto masks, including phi6 bacteriophage, HSV-1, CVB3, and SARS-CoV-2. Given that SARS-CoV-2 is transmitted via expired respiratory droplets and aerosols, it is critical to address respirator safety for reuse. This study provided experimental validation of a suitable aHP treatment process that decontaminates the respirators while maintaining N95 function. After ten rounds of aHP treatment, respirators passed N95 filtration efficiency testing. Virus inactivation by aHP was comparable to the sterilization of commercial spore-based biological indicators. These data demonstrate that the aHP process is effective, on the basis of zero failure rate on fit-testing of respirators, effective decontamination of multiple virus species including SARS-CoV-2, successful sterilization of bacterial spores, and filtration efficiency maintained at or greater than 95%. Collectively, these studies support the use of specific aHP decontamination protocol that permits safe reuse of N95 respirators by healthcare providers.

Importance

The ongoing COVID-19 pandemic has led to unprecedented pressure on healthcare and research facilities to provide adequate personal protective equipment. Given that the current pandemic is caused by a respiratory viral pathogen, the availability of highly protective respirator facepieces is critical to limit inhalation of this virus. While respirator facepieces were designed for single-use and disposal, the pandemic has increased overall demand for N95 respirators, and corresponding manufacturing and supply chain limitations have necessitated the safe reuse of respirators when necessary. The biosafety level 3 (BSL3) facility used in this study regularly

utilizes aerosolized hydrogen peroxide (aHP) to decontaminate equipment and spaces. We repurposed this technology for N95 respirator decontamination during the COVID-19 pandemic. Results from virus inactivation, biological indicators, respirator fit testing, and filtration efficiency testing all indicated that the process was effective at rendering N95 respirator safe for reuse.

Keywords:

N95 respirators, decontamination, aerosolized hydrogen peroxide, COVID-19, SARS-CoV2, virologic testing, virus, fit-testing, disinfection, sterilization, Pathogo™ Curis®

Abbreviations:

aHP, aerosolized hydrogen peroxide (H_2O_2); BSL, biosafety level; COVID-19, coronavirus disease 2019; CVB3, coxsackievirus B3; H_2O_2, hydrogen peroxide; HPM, hydrogen peroxide vapor monitor; HSV-1, herpes simplex virus 1; phi6, *Pseudomonas* phi6 bacteriophage; OSHA, Occupational Safety and Health Administration; QLFT, qualitative fit test; QNFT, quantitative fit-test; SARS-CoV-2, severe acute respiratory syndrome coronavirus 2; VPHP, Vapor-phase hydrogen peroxide.

Introduction

In response to the ongoing severe acute respiratory syndrome coronavirus 2 (SARS-CoV-2) pandemic, there is a shortage of personal protective equipment (PPE). In healthcare settings, the need for PPE is critical to protect frontline healthcare providers from infection, and to reduce cross-contamination between patients with coronavirus disease 2019 (COVID-19) and other uninfected patients. In healthcare settings, N95 respirators (including surgical N95 respirators) are used to provide protection from airborne infectious particles. The N95 terminology refers to the ability to block at least 95 percent of the most penetrating particle sizes (0.1 - 0.3 micron). Proper use of N95 respirators requires qualitative fit-testing (QLFT) or quantitative fit-testing (QNFT), which are designed to ensure a tight face-to-respirator seal for each specific wearer's face.

58 The current shortage of N95 respirators is due to limitations on the required raw materials,
59 limited capacity to manufacture the masks, and the ability of supply and distribution chains to
60 handle increased global demand. For this reason, researchers have sought to demonstrate the
61 potential for decontamination and reuse of existing N95 respirators. Standardized procedures are
62 well-established for the sterilization and reuse of medical equipment, such as autoclaving, steam
63 treatment, and chemical inactivation (e.g. bleach) (1). Sterilization of most medical equipment is
64 verified using spore-based biological indicators (2). Unlike most hospital equipment (e.g. steel,
65 metal, plastic) or fabrics (e.g. blankets) for which standardized sterilization methods exist (1),
66 N95 respirators are generally not intended for re-use (3). Thus many of the standard sterilization
67 approaches deform, damage, or destroy the integrity of N95 respirator fabric, nosepiece
68 materials, or elastic straps (4, 5). Hydrogen peroxide (H_2O_2)-based methods have been
69 successfully adapted for use in decontamination of N95 respirators, with indications that these
70 methods are less damaging than other decontamination methods (e.g. chemical or steam), and
71 can penetrate the densely-woven fabric of respirator facepieces (4, 6). In addition, the viricidal
72 capability of H_2O_2 sterilization methods has been previously demonstrated (7–9). Vapor-phase
73 H_2O_2 methods (e.g. "VHP" and other patented methods) have been used to decontaminate N95
74 respirators and were granted U.S. Food and Drug Administration (FDA) "Emergency Use
75 Authorization" (EUA) for healthcare use; however, these methods employ high concentrations of
76 hydrogen peroxide (30-70%) and elevated temperature to achieve vaporization. Vapor-phase
77 H_2O_2 (VPHP) methods at these concentrations pose increased health risks to decontamination
78 personnel, and combined with elevated temperature, can result in notable respirator material
79 decay (10). Historical aerosolized H_2O_2 (aHP) methods utilize lower peroxide concentrations (5-
80 6%) with silver ions and other antimicrobial agents, activated aerosolization via plasma, nozzle
81 pressure, or ultrasound, with similar limitations to VPHP methods (11–15). These methods have
82 not received strong comparative support in U.S. markets due to lower sterilization effectiveness
83 (13, 15–21). Therefore, we utilized a recently developed aHP method (i.e. the Pathogo™ Curis®
84 system), which dispenses a low concentration hydrogen peroxide solution through a precision
85 adjustable nozzle. The unit design and decontamination process characteristics allow consistent
86 distribution of disinfectant over time and effective decontamination of space and materials with
87 reduced health risk to personnel (22).

88 At present, respirator manufacturers have not approved protocols for N95 respirator
89 decontamination (3). To address imminent pandemic needs, healthcare settings are referencing
90 U.S. Centers for Disease Control and Prevention (CDC) guidelines on provisional N95 respirator
91 decontamination and reuse (22). Battelle Memorial Institute of Columbus, Ohio, received FDA
92 EUA status for an N95 decontamination protocol using a VHP method, based on a prior study
93 addressing the potential for respirator reuse in emergency scenarios (4, 23). This study included
94 evaluation of respirator structure, filtration, and manikin fit-testing, and used bacterial spore-
95 based biological indicators to demonstrate effective sterilization (4); however, viral inactivation
96 testing and respirator fit on live subjects were not performed. Given the current pandemic entails
97 a respiratory viral pathogen, several decontamination protocols are being actively investigated at
98 research universities and medical centers (24–31).

99 Given the reduced personnel health risks of using aHP, we assessed the ability of an aHP
100 decontamination protocol to achieve viral and microbial sterilization of N95 respirators, while
101 preserving respirator fit and integrity over multiple treatment cycles. Several respirator facepiece
102 types, representing those in use by local healthcare and research personnel, were included, and
103 decontamination was tested using multiple viral surrogates representing the structure,
104 characteristics, and environmental resistance of the SARS-CoV-2 pathogen. These surrogates
105 included *Pseudomonas* phi6 bacteriophage (phi6), herpes simplex virus 1 (HSV-1), and
106 coxsackievirus B3 (CVB3). After establishing successful decontamination of these surrogate
107 virus species, we further demonstrated decontamination of infectious SARS-CoV-2 virus spotted
108 on to respirators. Throughout the process, *Geobacillus stearothermophilus* spore-based
109 biological indicators were used to verify effectiveness of decontamination. Testing of virus
110 inactivation utilized plaque or tissue culture infectious dose 50% (TCID50) assays to detect the
111 partial inactivation of viruses by drying or desiccation onto respirator surfaces, and their
112 subsequent decontamination by aHP. Fitness of respirators for reuse was assessed by qualitative
113 and quantitative respirator fit testing of subjects using respirators subjected to multiple
114 decontamination cycles. Real-time measurement and separate diffusion sampler analyses of
115 hydrogen peroxide were used to monitor aHP levels associated with decontamination and
116 subsequent decomposition of aHP through drying prior to fit testing and reuse.

Methods

Decontamination Facility

The decontamination process was carried out in the Eva J. Pell Laboratory for Advanced Biological Research at The Pennsylvania State University, University Park campus. This facility is a purpose-built BSL3 enhanced facility, and all required approvals were obtained from the Institutional Biosafety Committee (IBC) for work involving viruses, as described below.

The primary decontamination process was performed within in an approximate 1,700 cubic feet sealed Preparation Room (Prep Room), followed by additional virus inactivation testing with SARS-CoV-2 in a separate, nearby 1,840 cubic feet Prep Room. Procedures and personal protective equipment (PPE) suitable for the viruses and materials in use were strictly observed in this biosafety level 3 (BSL-3) facility, which has consistently maintained institutional, CDC, and USDA approval for work with risk group 3 pathogens since its commissioning in 2014.

Decontamination Preparation

Respirators for decontamination were staged on a portable metal rack located centrally in the Prep Room (Supplementary Figure 1). Filtered and conditioned air is supplied to the Prep Room and the air exhausted from the room is HEPA-filtered. Bubble-tight dampers (Camfil Farr®) were operated to seal both the supply and exhaust air from associated ductwork during the decontamination cycle. The Curis® decontamination unit (Supplementary Figure 2) was programmed, equipment positioned, and the room doors sealed using polyethylene sheeting and non-porous adhesive tape (Supplementary Figure 3).

Decontamination Process

The Curis® decontamination unit programming method utilizes room size to establish the baseline parameters for charge (initial aHP dispensing) and intermittent aHP pulse periods. Once the user inputs the room's cubic volume or dimensions, the unit calculates the appropriate duration of the charge and pulse periods. Unit operation includes a user-defined dwell period (when no further aHP is introduced), at closure of the pulse period. Aeration is initiated following the dwell period (room seals are broken and ventilation resumed). The standard

145 aeration period is 3 hours, unless an auxiliary scavenging system is attached, or other space
146 aeration system is utilized.

147 Under air-tight/sealed conditions with neutral pressurization for the 1700 ft^3 room used,
148 programming included an 11-minute, 43-second continuous charge of aHP (7% H_2O_2;
149 Curoxide®), followed by six (6) pulse charges evenly spaced over 30 minutes to maintain H_2O_2
150 concentrations. To account for absorption of aHP into porous materials in the decontamination
151 space (e.g. N95 respirators), a 30-40% increase in these default settings was initially used, as is
152 typically recommended by the manufacturer. Additionally, to ensure adequate contact time of
153 disinfectant to the treated surfaces, a dwell period is recommended after the continuous and pulse
154 charge periods (decontamination phase) and prior to the aeration phase. Based on initial results,
155 adjustments in the charge, pulse, and dwell periods were conducted to establish effectiveness of
156 the overall decontamination process (Tables 3-4).

157 After completion of the decontamination phase, an aeration or dissipation phase was initiated by
158 removing fixed room seals and opening exhaust dampers for up to 2-hour periods, with the room
159 under slight vacuum (0.18-0.19" W.G.). Adjustments were made to room air exchange rate
160 during aeration to efficiently dissipate detectable H_2O_2 from respirator facepieces. At cycle 5,
161 final parameters were established to include an aeration exhaust rate greater than or equal to 35
162 air changes/hour, with make-up air supplied by outdoor air. Following this phase, and after room
163 H_2O_2 concentration was measured at less than 1 ppm, the respirator-holding rack was either
164 retained under ventilation or transferred to a separate room (referred to as the "Finishing Room")
165 with an HVAC air supply curtain to further dry and decompose residual aHP from respirator
166 facepieces to less than 1 ppm H_2O_2 (8, 9).

167 For respirators subjected to repeated rounds of decontamination as part of this study,
168 decontamination cycles were conducted repetitively from staging through drying. In order to be
169 considered "dry" or ready for the next cycle, the interior and exterior respirator surfaces were
170 monitored using a calibrated, hand-held real-time H_2O_2 monitor (ATI PortaSens II), and H_2O_2
171 concentrations were required to measure less than 1 ppm prior to repeating a cycle, or prior to
172 transport for subsequent respirator fit-testing or virus inactivation analysis. The U.S. Department
173 of Labor/Occupational Safety and Health Administration (OSHA) and the American Conference
174 of Governmental Industrial Hygienists (ACGIH) have established or adopted an eight-hour time-

175 weighted average (TWA) occupational permissible exposure limit (PEL) to hydrogen peroxide
176 of 1 ppm (32, 33). Though researchers and fit-test subjects were not anticipated to experience
177 this eight-hour exposure level, 1 ppm H_2O_2 concentration was used as a safety threshold for
178 room entry, sealing respirators for transport, and re-use by study participants.

179 Since this study did not involve respirator re-use in actual hospital or clinical settings for safety
180 reasons, the treated/dried respirators were subjected to manual stress as a proxy for the physical
181 wear during use that may challenge subsequent fit integrity. To simulate this stress condition,
182 each respirator was flexed bi-directionally and each band was stretched twice to a hold position
183 similar to respirator donning, prior to re-start of the next decontamination cycle.

184 Spore-based Biological Indicators

185 Biological indicator (BI) spore discs (Steris Spordex®) inoculated with Geobacillus
186 stearothermophilus (ATCC® 7953; mean spore count 2.4 x 10^5) were used to verify successful
187 decontamination (34). BIs (between 6 and 12 per cycle) enclosed in Tyvek/glassine envelopes
188 were placed throughout the room for each decontamination cycle. These were located behind or
189 beneath equipment and surfaces, on the portable metal rack holding respirators, and either on or
190 enclosed within the respirators themselves (Supplementary Figure 4). BIs were collected after
191 each cycle, each spore disc transferred from glassine/Tyvek envelopes to tryptic soy broth
192 (Spordex® Culture Media), incubated at 55°C, and analyzed after 7 days as an indicator of
193 effective decontamination (Supplementary Figure 5).

194 Chemical Indicators of H_2O_2

195 Chemical indicator strips (Steris Steraffirm® or Curis® System Hydrogen Peroxide Test Strips)
196 (between 1 and 4 total per cycle) were placed in various locations throughout the Prep Room to
197 indicate the presence of H_2O_2, supporting successful decontamination.

198 Real-Time Hydrogen Peroxide Monitoring

199 The portable ATI PortaSens II detector (PortaSens) was used to measure H_2O_2 levels both within
200 and outside the Prep Room during the decontamination process. Hydrogen peroxide
201 concentrations were measured at respirator surfaces, and necessarily reduced to less than 1 ppm
202 prior to handling or sealing for transportation to designated tissue culture rooms. During the

203 charge and pulse periods of decontamination, real-time instantaneous sampling was conducted
204 through a sealable wall port (designed for sterilizer tubing) into the Prep Room. The PortaSens
205 was also used to monitor Prep Room concentrations at the start of the aeration phase, and to
206 verify concentrations were reduced to less than 1 ppm for safe re-entry to the room (without
207 respiratory protection). In addition, H_2O_2 concentrations were also monitored within the adjacent
208 corridor along the Prep Room door seal (see Supplementary Figure 3), to assess H_2O_2 leakage.

209 Hydrogen Peroxide Diffusion Samplers (H_2O_2 Vapor Monitors)

210 Diffusion samplers, also known as hydrogen peroxide vapor monitors (HPMs) were utilized to
211 monitor long-duration H_2O_2 leakage outside the Prep Room entry (outside containment or OC),
212 on research personnel during decontamination activities (breathing zone samples, clipped to
213 lapel-collar), and within sealed respirator transport containers (prior to fit-testing) to verify that
214 H_2O_2 concentrations remained less than 1 ppm throughout transport and fit-testing. Once the
215 decontamination process was standardized with specific room ventilation parameters, ongoing
216 personnel monitoring was discontinued.

217 HPM sampler analysis was conducted by Advanced Chemical Sensors, Inc. (ACS) of
218 Longwood, FL utilizing an ACS HP-10 hydrogen peroxide vapor monitor, via modified OSHA
219 Method VI-6 (colorimetric analysis). Analysis was subcontracted and completed by laboratories
220 participating in the American Industrial Hygiene Association (AIHA) Laboratory Accreditation
221 Program. The AIHA is an ISO/IEC 17025 accrediting body (35, 36).

222 Respirator Selection for the Study

223 The N95 respirator facepiece models examined in this study represent those frequently used at
224 Penn State or within the Penn State Health system. Six models were selected, with a range of
225 characteristics, including those identified as surgical N95 respirators (no exhalation valve to
226 maintain sterile field), and non-surgical N95 respirators with an exhalation valve. These
227 characteristics are summarized in Table 1 and illustrated visually in Supplementary Figure 6.
228 Respirator models were required to be successfully fitted by test subjects. Fit-testing participants
229 included experienced test subjects and/or administrators. Several respirator models were
230 qualitatively fit-tested (QLFT) using Occupational Safety and Health Administration (OSHA) fit
231 test protocols (saccharine challenge) described in the OSHA Respiratory Protection Standard (29

232 CFR 1910.134) (37). This included standard exercises to challenge respirator fit, over an
233 approximate 8 minute, 30 second period. Additionally, quantitative fit-testing (QNFT) was
234 conducted using OSHA protocol requirements with a T.S.I, Inc. PortaCount Pro+ Model 8038
235 Fit Tester. This latter method employs condensation nucleus or particle counting technology
236 (CNC or CPC) to measure aerosol concentration outside and inside the facepiece to determine a
237 user fit-factor (38).

238 Sample Size and Acceptance Criteria for Fit-Test Reliability

239 Study design for the QLFT endpoint was intended to rigorously evaluate user respirator to
240 facepiece seal with 3M 8511 respirators, while also providing representative feasibility data for
241 the other respirator models (Table 1). Sample sizes associated with additional respirator models
242 in Table 1 (i.e., those other than 3M 8511) were not derived to meet a statistical endpoint. The
243 3M 8511 respirators used in this study were procured and collected by Penn State from 2006 to
244 2009. As is common with stockpiled supplies, the manufacturer's 5-year expiration date had
245 been exceeded prior to this study for the 3M 8511 respirators. All other respirator models (Table
246 1) were tested prior to their expiration date. All respirator models were unused prior to this study.

247 Acceptance criteria for 3M 8511 respirators required a minimum sample of 59 facepieces with
248 no failures during QLFT in order to conclude with 95% confidence that at least 95% of 3M 8511
249 respirators maintain fit integrity after repeated use and decontamination. A total of seventy-seven
250 3M 8511 respirators were available for study purposes. A small number of these, as well as other
251 respirator models were allocated for QNFT and virology testing subsequent to fit testing rounds.
252 QNFT provided metric data related to fit factor, safety margin, and objective evaluation of the
253 QLFT process to detect user fatigue (e.g., false negative for saccharine challenge). The 63
254 remaining 3M 8511 respirators provided sufficient sample size for evaluation against our
255 acceptance criteria based on QLFT.

256 Respirator Fit-Testing

257 Prior to decontamination, respirators were labeled with a unique identifier. After
258 decontamination, a hash mark was placed on the lower elastic band of each respirator to identify
259 the round(s) of decontamination completed (Supplementary Figure 7). At the conclusion of aHP
260 decontamination, respirators were confirmed to have less than 1 ppm H_2O_2 before transfer into

261 sealed plastic containers for transport to the fit-testing facility. Since the study was conducted
262 during the COVID-19 pandemic, social distancing conditions limited the use of multiple test
263 subjects, therefore, two respirator fit-test subjects were selected (one male, one female) for fit-
264 testing of selected respirators. All 3M 8511 respirators were subjected to QLFT on the first, fifth,
265 and tenth rounds of decontamination. In order to continually monitor QLFT test outcomes on the
266 same facepieces over the course of sequential cycles of decontamination, a small number of
267 respirators per model were allocated for QNFT during each round of fit testing. Based on
268 historical studies by the QNFT device and respirator manufacturers, N95 respirators have
269 maximum breakthrough for particle sizes of 0.1 – 0.3 micron. Particles smaller or larger than this
270 range have increased filtration efficiency (greater than 95%). QNFT fit testing of N95 respirators
271 therefore focuses on measuring this maximum penetration size range, to ensure that detectable
272 leakage is due to facepiece seal leakage. OSHA has established a minimum QNFT passing fit
273 factor of 100 for half-face respirators (including N95s or filtering-facepiece respirators) (37).
274 The QNFT instrument manufacturer has established a maximum quantifiable fit factor of 200, as
275 limited by measurement reliability and particle counting factors. QNFT fit factors equal to or
276 exceeding 200 are therefore reported as 200(+). The reported QNFT data were utilized to verify
277 successful fit reported by QLFT.

278 Respirators subjected to QNFT (with metal grommet/probe installed) could not be reused for fit
279 testing. These were repurposed for subsequent virus inactivation testing in order to conserve
280 overall respirator use.

281 NIOSH Filtration Efficiency Testing

282 To determine whether N95 respirators used in this study experienced filtration media breakdown
283 as a result of sequential aHP disinfection cycles, several respirators were sent for independent
284 laboratory analysis. These included eight 3M 8511 respirators subjected to cyclic aHP treatment
285 and intermittent fit-testing, and two additional unused, untreated 3M 8511 respirators. Respirator
286 filtration efficiency testing was performed by ICS Laboratories, Inc. (ICS) of Brunswick, Ohio.
287 ICS is one of two firms in the U.S. authorized by the National Institute for Occupational Safety
288 and Health (NIOSH) to perform respirator certification or re-certification.

289 An abbreviated "short-cycle" filtration efficiency verification test was conducted using the
290 NIOSH Standard Test Procedure TEB-APR-STEP-0059 (39), which is summarized below. The

291 standard test protocol includes initial respirator conditioning at 85 +/- 5% relative humidity
292 (%RH) and 38 +/- 2°C for 25 hours prior to testing. This conditioning was intended to reflect
293 active moisture load created by the respirator user. Following sealing of the respirator exhalation
294 valve, and placing into the test instrument, full-load testing was performed. This testing included
295 respirator challenge using 200 milligrams sodium chloride aerosol (mean count particle size
296 distribution verified as 0.075 +/- 0.020 microns, with geometric standard deviation not exceeding
297 1.86). Sodium chloride aerosol was neutralized to a "Boltzman equilibrium state" (25 +/- 5°C, 30
298 +/- 10% relative humidity), and introduced at an airflow rate of 85 +/- 4 liters per minute, with
299 periodic check and adjustment to maintain this flowrate. Instrumental analysis was conducted
300 using a T.S.I Automated Filter Tester Model 8130A. Recorded data included flow rate,
301 resistance, penetration, maximum penetration and filtration efficiency.

302 The test protocol establishes the means for ensuring that the particulate filtering efficiency of
303 N95 series filters used on non-powered respirators submitted for Approval, Extension of
304 Approval, or examined during Certified Product Audits, meets the minimum certification
305 standards set forth in 42 CFR, Part 84, Subpart K, §84.181.

306 **Virus Inoculation and Titration**

307 Viruses used here included herpes simplex virus 1 (HSV-1) strain F, coxsackievirus B3 (CVB3),
308 *Pseudomonas* phi6 bacteriophage (phi6) and SARS-CoV-2 isolate USA-WA1/2020. The key
309 characteristics of these viruses are summarized in Table 2. All virus-inoculated materials were
310 handled in accordance with the biosafety level (BSL) specified for that virus (see Table 2). In all
311 numbered aHP cycles (Table 4), the respirators used for virus inactivation testing had been
312 subjected to preceding total number of aHP cycles – e.g. respirators used for viral testing in aHP
313 cycle #6 had been already been subjected to 5 prior aHP cycles. In the case of the aHP cycles
314 labeled "Post" (i.e. Post 1, 2, or 3, which took place in a second Prep Room; see Table 3), the
315 respirators used had all been through between 10-12 prior aHP cycles. In all cases, the input
316 inoculum for each virus was set to the maximum available in each viral stock preparation.

317 For virus inactivation testing, respirator facepieces were inoculated with a controlled amount of
318 one or more surrogate virus species (refer to Table 2 for complete list). Each virus was added in
319 duplicate (or in quadruplicate during "Post 1-3" cycles of testing) droplets of 10 µL each, on one
320 or more surfaces of each respirator type. Droplets were allowed to air-dry or absorb fully onto

321 each respirator inside a Class II biosafety cabinet (BSC), before proceeding further. Selected
322 samples of each virus-inoculated respirator were left open to air, without aHP decontamination,
323 as a "drying-only" virus control. The remainder of each virus-inoculated facepiece was subjected
324 to aHP decontamination as described above (i.e. "decontaminated" samples). For each round of
325 viral testing, the duration of air-drying was matched to the duration of time needed for aHP
326 treatment of parallel respirators (i.e. including transport, respirator staging in the Prep Room,
327 aHP decontamination, aeration, and return to the viral testing location). After aHP treatment,
328 respirators, each virus-inoculated area was sliced out of the "dried" or "decontaminated"
329 respirators using dissection scissors. Each excised virus-spot encompassed all layers of the
330 respirator, to capture any virus that had absorbed beyond the surface fabric.

331 Herpes simplex virus 1 and coxsackievirus B3 quantification

332 Respirator areas inoculated with HSV-1 or CVB3 were transferred into individual Eppendorf
333 tubes and resuspended in a 250 µL volume of cell media. Cell media consisted of Dulbecco's
334 Modified Eagle's Medium (DMEM) supplemented with 10% fetal bovine serum (FBS) and
335 penicillin-streptomycin (Pen/Strep; 100 U/mL; Thermo Fisher Scientific). The number of
336 infectious units, or plaque-forming units (PFU), for these viruses was determined by limiting
337 dilution onto confluent Vero detector cell monolayers (*Cercopithecus aethiops* monkey kidney
338 cells, ATCC® CCL-81™). Plaque formation was assessed at 72 hours post infection (hpi), after
339 fixation and visualization of plaques using methylene blue staining (Figure 3). Duplicates of each
340 virus-inoculated respirator piece were frozen for titration at a subsequent date, separate from the
341 initial viral quantification. This allowed for experimental redundancy in terms of detector cell
342 monolayers, and reduced handling time for the large numbers of virus-respirator inoculation
343 sites.

344 Bacteriophage phi6 quantification

345 Respirator areas inoculated with phi6 bacteriophage were resuspended in 250 µL of King's
346 medium B (KB). These were then quantified on lawns of *Pseudomonas syringae pathovar*
347 *phaseolicola* strain 1448A (*Pph*) using a previously described soft agar overlay protocol (40).
348 Briefly, 100 µl logarithmic culture of *Pph* (OD_{600} ~ 0.5) and 100 µl of the phage preparation
349 were sequentially added to 3 ml of molten soft agar (0.7%) maintained at 55ºC. The mixture was
350 quickly poured on top of a KB agar plate and dried in the biosafety cabinet before transferring to

351 a 28ºC incubator. Alternatively, for enumeration of "inoculum" and "dried" samples, soft agar
352 *Pph* lawns were prepared and 10 µl dilutions of phage preparation were spotted (Figure 1).
353 Plaque forming units (PFU) were enumerated after 24-48 hours of incubation at 28ºC.

354 **SARS-CoV-2 quantification**

355 All experiments with SARS-CoV-2 were conducted in the Pell Laboratory under biosafety level
356 3 (BSL3) enhanced conditions using the USA-WA1/2020 isolate. SARS-CoV-2 was spotted onto
357 masks in quadruplicate and treated with aHP. After aHP treatment, Respirator areas inoculated
358 with SARS-CoV-2 were excised and resuspended in 250 µL of DMEM supplemented with
359 sodium pyruvate, non-essential amino acids, antibiotics-antimycotics, and 2% FBS. After
360 resuspension, viral titer was determined by tissue culture infectious dose 50 (TCID50) assay in
361 96-well plates, using Vero E6 cells. Briefly, 20 µL of resuspended sample was added to 4 wells
362 containing 180 µL of resuspension media. The added samples were then serially diluted 10-fold
363 down the plate, and the plates were incubated at 37 ºC for 96-hours. At this time, cytopathic
364 effect (CPE) was scored, and titer was calculated using the method of Reed and Muench (41).

365 # Results

366 **Chemical Verification and Biological Validation of Aerosolized H_2O_2 Process**

367 This study was intended to rigorously evaluate a protocol for decontamination and re-use of N95
368 respirators using aerosolized hydrogen peroxide (aHP) treatment. The study focused
369 predominantly on the 3M 8511 respirator, while also extending this approach to other respirator
370 models (Table 1). The decontamination process was performed in the BSL3 enhanced facility,
371 enabling the assessment of inactivation of viruses spanning multiple biosafety levels, including
372 SARS-CoV-2 (Table 2). As described above (in Methods), the final aHP decontamination
373 process involved a "charge period" (initial aHP injection), followed by a "pulse period"
374 (intermittent aerosol injection for six intervals of 5-minutes each, after completion of the initial
375 charge period), and a final 20-minute "dwell period" or quiescent maintenance of the aHP room
376 conditions. Upon completion of the "dwell period", an aeration phase was initiated to evacuate
377 aHP from the room. Importantly, the aHP method used for decontamination was adapted from
378 that used to decontaminate solid equipment, to allow for the absorbent nature of N95 respirators.
379 The charge, pulse, and dwell period parameters were adjusted to optimize cycle times (Table 3)

380 as well as to account for biological indicator and virology results. Our initial tests utilized a 40-
381 minute pulse period with no dwell time (Table 3: "Initial" parameters), which was reduced to 30
382 minutes in subsequent runs ("Modification 1") to optimize overall cycle time and reduce residual
383 H_2O_2 on respirator surfaces. Upon minor failures of biological indicators and viral inactivation
384 (see below and Table 4), we incorporated a 20-minute dwell period to enhance inactivation
385 without increasing H_2O_2 concentrations (Table 3: "Final" parameters).

386 All chemical indicators located throughout the decontamination area (Prep Room) during all aHP
387 cycles revealed exposure to hydrogen peroxide. For cycles in which charge, pulse, and dwell
388 periods were utilized, all biological indicators similarly indicated successful decontamination,
389 with the exception of aHP cycles 3 and 5 (Table 4). In cycle 3 the additional dwell period was
390 not yet implemented, and BIs indicated an unsuccessful decontamination cycle (1 positive; 5
391 negative). During transfer of spore coupons to media after treatment cycle 5, it was noted that
392 external contamination of one spore coupon may have occurred, potentially resulting in the
393 single positive indicator for this specific BI. Overall, chemical and biological indicator results
394 supported aHP treatment and decontamination of N95 respirators with the room and cycle
395 parameters utilized in this study.

396 Real-Time Hydrogen Peroxide Monitoring

397 Real-time H_2O_2 measurement concentrations during the decontamination process were obtained
398 with a portable, real-time ATI PortaSens II monitor (summarized in Table 5). Instantaneous
399 H_2O_2 concentrations in the treatment area (inside containment or IC) were measured at $\geq$ 120
400 ppm during the charge and pulse periods. Hydrogen peroxide concentrations in the corridor
401 outside the sealed entryway (outside containment or OC) were low or undetected (0 ppm)
402 throughout the decontamination cycle; however, occasional concentrations were detected up to 3
403 ppm. These detectable levels were consistently associated with broken seals in the tape around
404 the door, and when corrected, immediately reduced aHP levels to 0 ppm.

405 At the timed start of the aeration phase, tape seals at the door entry were removed, and the door
406 was opened and left slightly ajar. Hydrogen peroxide concentrations at the door were
407 subsequently monitored at breathing zone height (BZH) or 5 feet above floor level, until
408 concentrations measured $\leq$ 2 ppm. At this time research personnel entered the Prep Room to
409 measure H_2O_2 concentrations at respirator surfaces. Hydrogen peroxide concentrations were

410 observed to decline rapidly during aeration within 20-30 minutes of door opening. Initial
411 respirator surface concentrations (at fabric) typically exceeded 2 ppm. Subsequent respirator
412 drying to achieve < 1 ppm required further staging under aeration (exhaust ventilation)
413 exceeding two hours, or overnight. Once H_2O_2 respirator surface concentrations were measured
414 < 1 ppm, they were either subjected to further rounds of aHP, or collected and containerized for
415 further fit-testing or virus inactivation analysis.

416 Hydrogen Peroxide Diffusion Sampler (Monitor) Analysis

417 Diffusion samplers, also known as hydrogen peroxide vapor monitors (HPMs) were utilized to
418 assess researcher exposure levels to H_2O_2, with reference to the OSHA permissible exposure
419 limit (PEL) and ACGIH Threshold Limit Value (TLV®) of 1 ppm, as an eight-hour time-
420 weighted average (TWA). HPMs were also collected to monitor H_2O_2build-up within respirator
421 containers prior to fit-testing (for test subject safety), and to verify that H_2O_2 concentrations
422 remained low in areas occupied by researchers (outside containment) during the decontamination
423 process (summarized in Table 6). All personal breathing zone HPM sampler results were
424 reported below sample detection limits (< 0.08 ppm, <0.1 ppm) for researchers conducting all
425 aHP processing activities (up to 3 hours). All results for HPMs placed within sealed respirator
426 transport containers were reported below sample detection limits (< 0.03 ppm), indicating no
427 residual H_2O_2 present through transport and respirator fit-testing. All results for HPMs collected
428 as OC samples were reported below sample detection limits (< 0.08 ppm, cycle 1b) and < 0.2
429 ppm (cycle 11).

430 Qualitative and Quantitative Fit-Testing After aHP Decontamination

431 Fit-testing using both QLFT and QNFT on all 3M model 8511 respirators was assessed after the
432 first, fifth, and tenth decontamination cycles for both the male and female subject (summarized
433 in Figure 1). All respirators passed these fit tests. No other failures occurred, therefore with 95%
434 confidence, at least 95% of 3M model 8511 respirators maintain successful N95 fit seal after ten
435 aHP decontamination cycles based on these data. QNFT results associated with 3M model 8511
436 respirators passed the minimum passing fit factor of 100, and the maximum quantifiable fit
437 factor of 200(+) in 8 of 9 tests. The numerical range of passing fit factors (100 – 200), and
438 available sample quantity, limit statistical analysis. The consistently successful QNFT results

verified QLFT findings, and support retention of successful respirator fitting following repeated cycles of aHP decontamination and physical respirator stress.

QLFT and QNFT were also conducted on a smaller number of additional respirator models (as indicated in Table 1 and Figure 1). For these respirator models, a maximum of 11 facepieces were included, with all subjected to QLFT and a subset used for QNFT at various intervals. Respirator models 3M 1860, 3M 1870+, 3M 9211+, Kimberly Clark PFR95, and Sperian N1125 passed all QLFT and QNFT tests. One respirator facepiece (3M model 1870+) experienced a broken rubber strap when subjected to physical stress (e.g., stretching) after eight cycles of aHP. This respirator was treated as a censored observation since it had successfully passed QLFT after the first and fifth decontamination cycles but could not be fit-tested to assess fit seal and filtration performance after the tenth cycle. Since fit test results varied widely by subject during early testing of Alpha ProTech respirators, this model was discontinued from further study. Given that no respirator models included in this study were designed for reuse, any apparent shortcoming should not be interpreted as a failure of respirator performance when respirators are used as designed and intended by the manufacturer.

Respirator Filtration Efficiency Testing

N95 respirator filtration efficiency testing was conducted on stockpiled 3M 8511 aHP-treated respirators using the NIOSH test protocol under full-load test conditions (Table 7). No visible degradation was found on inspection (e.g. metal nose guard discoloration, unusual thinning or wear). Filtration efficiencies were found to exceed 95% for all eight respirators subjected to ten cycles of aHP decontamination. Therefore, for at least ten aHP cycles, there were no adverse impacts or loss of N95 respirator efficiencies. Two additional unused, untreated 3M 8511 respirators were additionally tested and found with slightly reduced filtration efficiencies (94.4%, 94.6%). These findings are consistent with the respirator manufacturer's 5-year shelf life limitation; however, the overall respirator performance is maintained.

Application of Multiple Viral Species to N95 Respirator Facepieces

Viral inactivation on respirator facepieces was anticipated to occur both by the process of drying or desiccation, and by the process of aHP decontamination. Multiple virus species were included to test the decontamination potential of aHP against viruses in general, as well as against SARS-

468 CoV-2. These included: *Pseudomonas* phi6 bacteriophage (phi6), herpes simplex virus 1 (HSV-
469 1) strain F, coxsackievirus B3 (CVB3), and SARS-CoV-2 isolate USA-WA1/2020 (see Table 2
470 for details). In order to preserve overall respirator consumption during the pandemic, respirators
471 used for virus inactivation testing were ones previously subjected to aHP treatment and fit-
472 testing (see Methods for details). Initial application of virus to each of the four (4) 3M respirator
473 facepiece types revealed clear differences in relative absorption vs. fluid repulsion. 3M respirator
474 models 1870+ and 9211+ share a common outer fabric which is listed by the manufacturer as
475 having the highest fluid resistance of any N95 respirator (42). In our testing, these two respirator
476 models displayed no apparent absorption of virus inoculum in our tests, and instead dried with a
477 "coffee ring effect" on the respirator surface. In contrast, all other respirator types (Table 1)
478 experienced a combination of liquid spreading, absorption, and evaporative drying of the virus
479 inoculum droplet. Viruses were inoculated onto different areas of each respirator facepiece
480 model, including the outer and inner fabric surfaces, the elastic strap, and where present, the
481 inner and outer surface of the plastic exhalation valves (see Supplementary Figure 6).

482 **Inactivation of Multiple Viral Species by Air-Drying on Respirators**

483 To mimic the potential inactivation of viruses that could occur during a multi-hour session of
484 respirator use, we tested the amount of virus remaining after air-drying of virus applied to N95
485 respirators. For each round of viral testing, the duration of air-drying was matched to the
486 duration of time needed for aHP treatment of parallel virus-inoculated respirator areas (see Table
487 4 for summary; detailed further below). These "drying-only" samples confirmed a partial loss of
488 viral infectiousness, ranging from 10-100-fold for phi6 and HSV-1, and 100-fold or greater for
489 CVB3 and SARS-CoV-2 (Figures 2-5; see also Supplementary Figure 8 and Supplementary
490 Table 1). For phi6 bacteriophage, this included 29 "drying-only" inoculation sites spanning three
491 independent rounds of testing (Figure 2). For HSV-1 and CVB3, this included 55 "drying-only"
492 inoculation sites for each virus species, spanning four independent rounds of testing (Figure 3
493 and Figure 4, respectively). Viral inactivation by drying was not markedly different on inner vs.
494 outer surfaces of the respirator models (Figures 2-5; see also Supplementary Table 1), or in
495 limited testing of alternative inoculation sites, such as elastic straps or plastic exhalation valves
496 (Figure 3A-B and Figure 4A-B).

497 **Decontamination of Virus-Inoculated Respirators by Aerosolized H_2O_2 Treatment**

498 While natural inactivation of viruses by air drying is an ancillary benefit of extended respirator
499 use, our main goal was to assess the effectiveness of active decontamination by aHP treatment.
500 For this purpose, parallel virus inoculation sites to those used in the air-drying experiments
501 above were subjected to aHP treatment, using both "Modification 1" and "Final" parameters (see
502 Table 3 for details). Viral testing of decontamination was conducted during six independent aHP
503 cycles (summarized in Table 4), using the maximum inoculum titer available for each viral stock
504 preparation. For phi6 bacteriophage, this included 37 "aHP-treated" sites spanning three
505 independent rounds of testing (Figure 2). For HSV-1 and CVB3, this included 65 and 63 "aHP-
506 treated" sites respectively, spanning four independent rounds of testing (Figure 3 and Figure 4).
507 Across a total of 213 respirator sites inoculated with one of four virus species tested (Table 2; see
508 also Supplementary Table 1), only 5 sites had any remaining infectious virus. Even these rare
509 instances of virus positivity still entailed a 4-6 $\log_{10}$ reduction in viral load from the initial
510 inoculum (10^6 reduction for phi6, Figure 2B; 10^5 reduction for HSV-1, Figure 3A; 10^4 reduction
511 for CVB3; Figure 4A-B). Three of these rare positive virus plaques were detected in an aHP
512 cycle using the "Modification 1" parameters (Figure 2A and 3A; Table 4; see also
513 Supplementary Figure 8), and these were a key motivation to add a dwell time in the "Final" aHP
514 cycle parameters (Table 3). There was no observable difference in the effectiveness of aHP
515 decontamination for inner vs. outer surfaces of respirators (Figures 2-5; see also Supplementary
516 Table 1), or in limited testing of alternative inoculation sites such as elastic straps (Figure 3A-B
517 and Figure 4A-B). The success of virus inactivation by aHP treatment mirrored the results of
518 biological indicators (BIs) consisting of bacterial spore coupons (Table 4).

519 **Inactivation of SARS-CoV-2 by aHP Treatment**

520 Experimental testing of SARS-CoV-2 by aHP necessitated that all work be completed at BSL3.
521 These studies were conducted with the 3M 8511, 1860, and 1870+ N95 respirators, spanning two
522 independent rounds of testing (Figure 5). As with the surrogate virus species, SARS-CoV-2 was
523 first inoculated onto respirator facepieces. The "drying only" controls were left open to air, while
524 the decontaminated samples were subjected to aHP-treatment. The respirators used for SARS-
525 CoV-2 testing had been subjected to 10 prior rounds of aHP before virus inoculation. For SARS-
526 CoV-2, viral testing included 48 "drying-only" inoculation sites and 48 "aHP-treated" sites,
527 spanning two independent rounds of testing (Figure 4). We observed a partial loss of viral

528 infectiousness for SARS-CoV-2 due to drying (e.g. $10^{6.125}$ TCID50/mL input vs ~10^2
529 TCID50/mL after drying; Figure 5). Importantly, no infectious SARS-CoV-2 remained on any
530 respirator model after aHP decontamination (Figure 5).

531 Discussion

532 Based on a series of ten respirator decontamination cycles and multiple rounds of viral
533 inactivation testing, 3M 8511 and other similar N95 respirator models tested were found to be
534 suitable for aHP decontamination and reuse. We found that respirators could successfully pass
535 qualitative respirator fit testing through multiple cycles of the aHP decontamination process, and
536 ultimately passed filtration efficiency tests indicating no loss in filtration efficiency. Most studies
537 thus far have focused either on verifying fit-testing after respirator decontamination (6, 27, 30),
538 or the ability of decontamination approaches to inactivate one or more virus species on
539 respirators (25, 29, 31), but not both. A minority of N95 respirator decontamination studies have
540 included both fit-testing and measures of viral inactivation (26, 28), although none have
541 employed the aerosolized H_2O_2 method utilized here. Our study is unique in including multiple
542 measures of respirator integrity via fit-testing, as well as filtration efficiency, and robust
543 verification of viral inactivation using multiple surrogates and SARS-CoV-2 itself. The breadth
544 of this approach will extend the usefulness of this study beyond the current pandemic.

545 Respirator Resilience for Re-Use

546 Aerosolized H_2O_2 decontamination of the N95 respirators used in this study did not indicate any
547 adverse impact on final respirator filtration efficiency. Hydrogen peroxide concentrations were
548 controlled within the study, supporting effective microbial and viral decontamination, with
549 proper containment of aHP and with no detectable researcher exposure. These findings support
550 and reflect those of parallel studies using other forms of hydrogen peroxide vapor, and/or other
551 decontamination methods for N95 respirators (24, 26–28, 30). In order to assess the H_2O_2
552 concentration profile during aHP decontamination (inside containment), and for comparison with
553 levels for different H_2O_2 decontamination methods, further studies would require use of real-time
554 instruments with a higher detection range and data logging features.

555 We are not aware of any studies reaching the ten cycles of aHP decontamination, with successful
556 fit-testing and verification of viral inactivation. As noted by the CDC, laboratory study

557 conditions such as those used in this study do not fully reflect clinical use conditions, which can
558 impact respirator fit and performance (43). While each facepiece was physically stressed
559 between each decontamination cycle as a proxy for use, then re-used by the same subjects during
560 fit-testing, sustained clinical use includes other pertinent stressors which may influence fit and
561 performance (e.g. build-up of facial oils, cosmetics, exhaled moisture, perspiration, intermittent
562 user adjustments) (27, 28, 43). Future studies are needed to explore these impacts during re-use,
563 in combination with the metrics used in this study.

564 During this study, one 3M 1870+ respirator suffered a broken rubber strap during re-use. The
565 breakage occurred after eight cycles of aHP, during inter-cycle strap stretching to simulate re-
566 use. The breakage occurred at a point on the strap that corresponded with a penned hash mark
567 (used to denote decontamination cycle; see Supplementary Figure 7). There were no other
568 instances of failure for this or any other respirator models. This observation has relevance to real-
569 world decontamination scenarios, in which elastic or rubber straps may be damaged with cycle
570 marking. Care should be exercised when marking respirators during re-use protocols, and a
571 visual inspection for incidental damage is prudent.

572 **Viral and Biological Indicator Inactivation**

573 To model real-world scenarios in which healthcare staff may have aerosolized virus absorbed on
574 to their respirator, we inoculated viruses onto different respirator surfaces to thoroughly test for
575 the ability of aHP to inactivate viruses. We further tested several different components and
576 regions of the respirator to discern whether any differences in respirator construction (e.g. outer
577 vs. inner surface fabric) would influence viral inactivation. This work was inspired by early
578 efforts to verify viral inactivation in the context of N95 respirator surfaces, such as that of
579 Kenney et al. (25) We found no evidence of viral survival during the aHP decontamination
580 process. Relative to other similar studies using different decontamination methods to test viral
581 inactivation on N95 respirators, these data shown an equal or better inactivation of viruses in the
582 present study (25, 26, 28, 29, 31). During establishment of aHP cycle process parameters, we
583 observed a biological indicator test failure (positive result), and corresponding virology test
584 failure associated with cycle 3, in which no dwell period was used. Commercial bioindicator
585 tests have been relied upon for sterilization processes over several years (2, 34). These data
586 suggest that the use of commercial spore-based biological indicators during decontamination of

587 N95 respirators provides a useful predictor of success or failure for viral inactivation as well. In
588 this study, we tested up to ten cycles of aHP decontamination, which meets or exceeds current
589 FDA recommendations for N95 respirator re-use following vapor-phase H_2O_2 decontamination.
590 (25–30).

591 Like SARS-CoV-1, SARS-CoV-2 has a high level of environmental stability (44–48). In terms
592 of virion characteristics, SARS-CoV-2 has a lipid-enveloped virion of ~120 nm, with no
593 icosahedral capsid core. The lipid envelope encloses a single-stranded, linear, positive-sense
594 RNA genome (summarized in Table 2). We used multiple virus species to test the viral
595 inactivation capabilities of aHP decontamination. These viruses represented multiple
596 characteristics of human viral pathogens, with a range of virion and genome types and sizes, and
597 previously documented environmental stability (49–51). Virions of herpes simplex virus 1
598 (HSV-1) and *Pseudomonas* phi6 bacteriophage have a lipid envelope, with an underlying
599 icosahedral capsid core. In contrast, coxsackievirus B3 (CVB3) is a non-enveloped or naked
600 icosahedral capsid virus. Prior work has shown that naked-capsid viruses have a higher stability
601 than enveloped viruses, thus providing a useful test of aHP sterilization abilities (49–51). While
602 most viruses utilized in this study are mammalian viruses requiring analysis in mammalian cell
603 lines at biosafety level 2 (BSL2), phi6 can be assayed more flexibly, using rapid bacterial
604 cultures (24-hour turnaround) at biosafety level 1. Phi6 is a natural pathogen phage of
605 *Pseudomonas syringae pathovar phaseolicola*, which is itself a bacterial pathogen of green
606 beans. We found that all viral species examined in this study were effectively sterilized by aHP,
607 comparable to the decontamination observed with commercial spore-based biological indicators
608 of sterilization. Together, this combination of respirator fit testing and virus inactivation testing
609 indicate that aHP is a suitable decontamination process to enable reuse of N95 respirators during
610 the COVID-19 pandemic.

611 Virus inactivation data associated with respirator analyses are impacted by the effects of viral
612 drying on hydrophobic respirator surfaces (31). Overall effectiveness of viral inactivation can be
613 consistently demonstrated through aHP process; however, there is no way to fully separate the
614 effects of air drying from the impacts of aHP. Clinical exposure to SARS-CoV-2 or other viral
615 pathogens would likewise entail conditions that allow viral drying prior to decontamination
616 and/or respirator re-use (e.g. virus may dry onto a respirator in the course of a work-shift, or air-
617 dry during respirator bagging for decontamination or direct re-use). If anything, our "drying-

618 only" time frame was shorter than would likely occur in a clinical setting. This suggests that
619 emergency-protocols that involve respirator re-use after multiple days of drying, even without
620 aHP or other similar decontamination methods, are likely providing substantial levels of viral
621 inactivation (22, 43).

622 Acknowledgements

623 We appreciate the contributions of colleagues and scientists who provided intellectual input
624 and/or materials for this work. These include Joyce Jose, Susan Hafenstein, Anthony Schmitt,
625 Gregory Broussard, Michael Brignati, and Tim Simpson. We thank Dr. Paul Turner and his lab
626 for providing phi6 bacteriophage. We appreciate the contributions and support of Jim Crandall
627 and the Penn State Environmental Health and Safety staff, as well Theresa Engle and other
628 Occupational Medicine staff, who provided support in study implementation, and fit-testing. We
629 also thank Irene Miller as part of the Pell Lab decontamination staff, researchers, clinical staff, as
630 well as Neerav Goyal, Justin Soulier, and the healthcare providers of the Penn State Health
631 Milton S. Hershey Medical Center and College of Medicine.

632 This work was supported by the Pennsylvania State University. SARS-CoV-2 research in Dr.
633 Troy Sutton's laboratory was initiated by a seed grant from The Huck Institutes of Life Sciences
634 at Pennsylvania State University, and Dr. Sutton's research is further supported by the USDA
635 National Institute of Food and Agriculture, Hatch project 4605.

636

637 # Tables

638 **Table 1: N-95 respirator facepiece models included in this study**

Brand & model	# in study	Style	Type	Exhalation valve	Notes
3M 8511	77	molded	Non-surgical	yes	
3M 1860	10	molded	Surgical	no	
3M 1870+	11	folded	Surgical	no	Highest fluid resistance*
3M 9211+	12	folded	Non-surgical	yes	Same fabric as 1870+
Honeywell Sperian N11125	5	molded	Non-surgical	yes	
Alpha ProTech	65	folded	Surgical	No	

639 * Highest level of fluid resistance according to ASTM F1862 at 160 mm Hg (42).

640
641

642 **Table 2. Characteristics of virus species used to test inactivation by aerosolized**
643 **H2O2, as compared to SARS-CoV-2**

Virus species (abbreviation)	Diameter	Capsid / virion shape	Genome type, ~size*	Taxonomic family	Biosafety Level (BSL)
Severe acute respiratory syndrome coronavirus 2 (SARS-CoV-2)	120 nm	Enveloped, no icosahedral capsid	linear (+) ssRNA genome, ~30 kbp	*Coronaviridae*	BSL3
Herpes simplex virus 1 (HSV-1)	200 nm	Enveloped, icosahedral	linear dsDNA genome, ~152 kbp	*Herpesviridae*	BSL2
Coxsackie virus B3 (CVB3)	30 nm	Non-enveloped (naked), icosahedral	linear (+) ssRNA genome, ~7.4 kbp	*Picornaviridae*	BSL2
Pseudomonas phi6 bacteriophage (phi6)	85 nm	Enveloped, icosahedral	segmented, dsRNA genome, ~13.3 kbp	*Cystoviridae*	BSL1

644 *ds, double-stranded; ss, single-stranded; ssRNA genomes are either (+) positive sense or (-)
645 negative sense.
646

647 **Table 3: Optimization of aHP treatment parameters**

aHP Cycle #	Room Volume (ft^3)	Charge Period	Pulse Period	Dwell Period	aHP Parameter Set
1a	1700	16:20	40:00	0:00	Initial
1b	1700	16:20	40:00	0:00	Initial
2	1700	11:43	30:00	0:00	Modification 1
3	1700	11:43	30:00	0:00	Modification 1
4	1700	11:43	30:00	0:00	Modification 1
5	1700	11:43	30:00	20:00	Final
6	1700	11:43	30:00	20:00	Final
7	1700	11:43	30:00	20:00	Final
8	1700	11:43	30:00	20:00	Final
9	1700	11:43	30:00	20:00	Final
10	1700	11:43	30:00	20:00	Final
11	1700	11:43	30:00	20:00	Final
12	1700	11:43	30:00	20:00	Final
Post 1	1840	12:41	30:00	20:00	Final*
Post 2	1840	12:41	30:00	20:00	Final*
Post 3	1840	12:41	30:00	20:00	Final*

648 * These cycles were carried out in a larger preparation room, which necessitated adjustment to
649 the charge time to account for the larger room size

650

651

652 **Table 4: Spore-based Biological indicator (BI) and Virus Inactivation Results**

aHP Cycle #	aHP-treated Spore-based BIs	Control Spore-based BIs	Spore-based BI Results	aHP parameter set	Viruses Tested	Virus Inactivation Results
1a	12	1	PASS	Initial		
1b	12	1	PASS	Initial		
2	--	--	--	Modification 1		
3	6	1	FAIL (1+/5-)	Modification 1	phi6, HSV1, CVB3	3 of 64 sites positive
4	6	1	PASS	Modification 1		
5	6	1	FAIL*(1+/5-)*	Final		
6	6	1	PASS	Final	HSV1, CVB3	1 of 26 sites positive
7	6	1	PASS	Final		
8	6	1	PASS	Final		
9	6	1	PASS	Final		
10	6	1	PASS	Final		
11	6	1	PASS	Final	phi6, HSV1, CVB3	1 of 9 sites positive
12	6	1	PASS	Final		
Post 1	--	--	--	Final	phi6, HSV1, CVB3	0 of 66 sites positive
Post 2	12	1	PASS	Final	SARS-CoV-2	0 of 24 sites positive
Post 3	12	1	PASS	Final	SARS-CoV-2	0 of 24 sites positive

653 *In cycle 5, it was noted upon transfer of one spore coupon to media, post-treatment
654 contamination may have occurred.
655

656 **Table 5: Portable real-time H_2O_2 measurements, using ATI PortaSens II**

aHP Cycle ID	Measurement Location*	Measurement Condition	H_2O_2 Concentration or range (ppm)**	Time period to decayed concentration (minutes)	aHP Parameter set
1a	IC, wall port	Charge	> 120	--	Initial
1a	IC, wall port	Aeration, to entry	2.5 – 57	52	Initial
1b	IC, wall port	Charge	> 120	--	Initial
2	No data	No data	No data	No data	Modification 1
3	IC, door open	Aeration, to entry	1.5 – 11.6	20	Modification 1
3	IC, door open	Aeration, to respirator measurement	1.5 – 0.8	40	Modification 1
4	IC, door open	Aeration, to entry	2 – 10.6	20	Modification 1
4	respirator surface	After overnight drying	0 – 3	overnight	Modification 1
5	IC, wall port	Charge	> 120	--	Final
6	IC, wall port	Pulse	120	--	Final
6	respirator surface	After overnight drying	0	overnight	Final
7	IC, wall port	Charge	> 120	--	Final
7	OC, seal check(s)	Charge, Pulse, Dwell	0	--	Final
7	IC, door open	Aeration, to entry	2 – 7	27	Final
7	respirator surface	After overnight drying	0	overnight	Final
8	IC, wall port	Pulse	88	--	Final
9	IC, wall port	Charge	> 120	--	Final
9	IC, door open	Aeration, to entry	1.6 – 24	20	Final
9	respirator surface	Aeration, to respirator measurement	< 1	85	Final
10	OC, seal check	Pulse, door seal repair	0 – 1.6	--	Final
10	IC, door open	Aeration, to entry	1.3 – 15	32	Final
10	respirator surface	After overnight drying	< 1	overnight	Final
11	IC, door open	Aeration, to entry	1 – 13.6	35	Final
11	respirator surface	After overnight drying	< 1	overnight	Final
Post	respirator surface	Aeration to 1ppm, respirator data log	1 – 8.1	150	Final

657 * Measurement Location: IC – inside containment, (wall port) – through sealable wall port, (door open) –
658 door ajar after door seal removed, OC – outside containment, (seal check) – Prep Room door tape seal,
659 (respirator surface) – at respirator surface following room entry.
660 ** Low measurement value represents lowest concentration following concentration decay; high value
661 represents starting concentration (prior to decay).
662

663 **Table 6: Hydrogen peroxide diffusion sampler (HPM) data**

aHP Cycle ID	Sample Type	Location Notes*	H_2O_2 (ppm)**	Sampling Period (minutes)***
1a	Researcher A – personal breathing zone	Sampler at worker lapel; transit in all service areas	< 0.1	143
1b	Researcher B – personal breathing zone	Sampler at worker lapel; transit in all service areas	< 0.08	185
1b	area sample	Door Seal (OC), breathing zone height	< 0.08	183
1b	respirator container	3M 1860 (within brown paper bag)	< 0.03	461
1b	respirator container	3M 9211+ (bag)	< 0.03	518
1b	respirator container	Alpha Protech PFL (within brown paper bag)	< 0.03	497
1b	respirator container	Alpha Protech PFL (within brown paper bag)	< 0.03	510
11	area sample	Door Seal (OC), breathing zone height	< 0.2	110

664 *C (charge period), P (pulse period), D (dwell period), A (aeration phase)
665 ** "< Value" indicates sample analysis was below limit of quantitation (LOQ) based on sampler
666 diffusion rate and air volume collected. Time-weighted average (TWA) not calculated for results
667 reported <LOQ. The OSHA PEL and ACGIH TLV® exposure standard for hydrogen peroxide is
668 1ppm eight-hour TWA.
669 ***Sampling period varied by sampling objectives.
670
671

672 **Table 7: Respirator filtration efficiency testing results following 10 cycles of**
673 **aerosolized hydrogen peroxide decontamination**

Full-loading efficiencies – 3M Model 8511 (N95 respirator)*						
Sample ID**	Initial Test Flow Rate (LPM)	Initial Test Resistance (mmH_2O)	Initial Test Penetration (%)	Maximum Penetration (%)	Filter Efficiency*** (%)	Result
MS – 1	84	6.5	0.67	2.29	97.71	Pass
MS – 2	85	6.7	0.82	2.38	97.62	Pass
MS – 3	84	6.9	1.46	4.16	95.84	Pass
MS – 4	85	6.8	1.75	4.14	95.86	Pass
FS – 1	85	7.1	2.02	4.58	95.42	Pass
FS – 2	84	6.6	1.47	3.5	96.50	Pass
FS – 3	85	6.6	0.20	2.37	97.63	Pass
FS – 4	86	7.0	1.47	4.12	95.88	Pass
Test specification	81-89			≤ 5.0	≥ 95.0	

674 * Respirator testing analysis performed by ICS Laboratories of Brunswick, OH
675 ** MS, FS – [x]Male subject or female subject sample respirator id
676 ***Filter efficiency percent is based on maximum penetration value.

677 # Figures

678

679 **Figure 1: Sequential fit testing (QLFT & QNFT) of N95 respirators subjected to**
680 **repeated aHP decontamination cycles.**

681

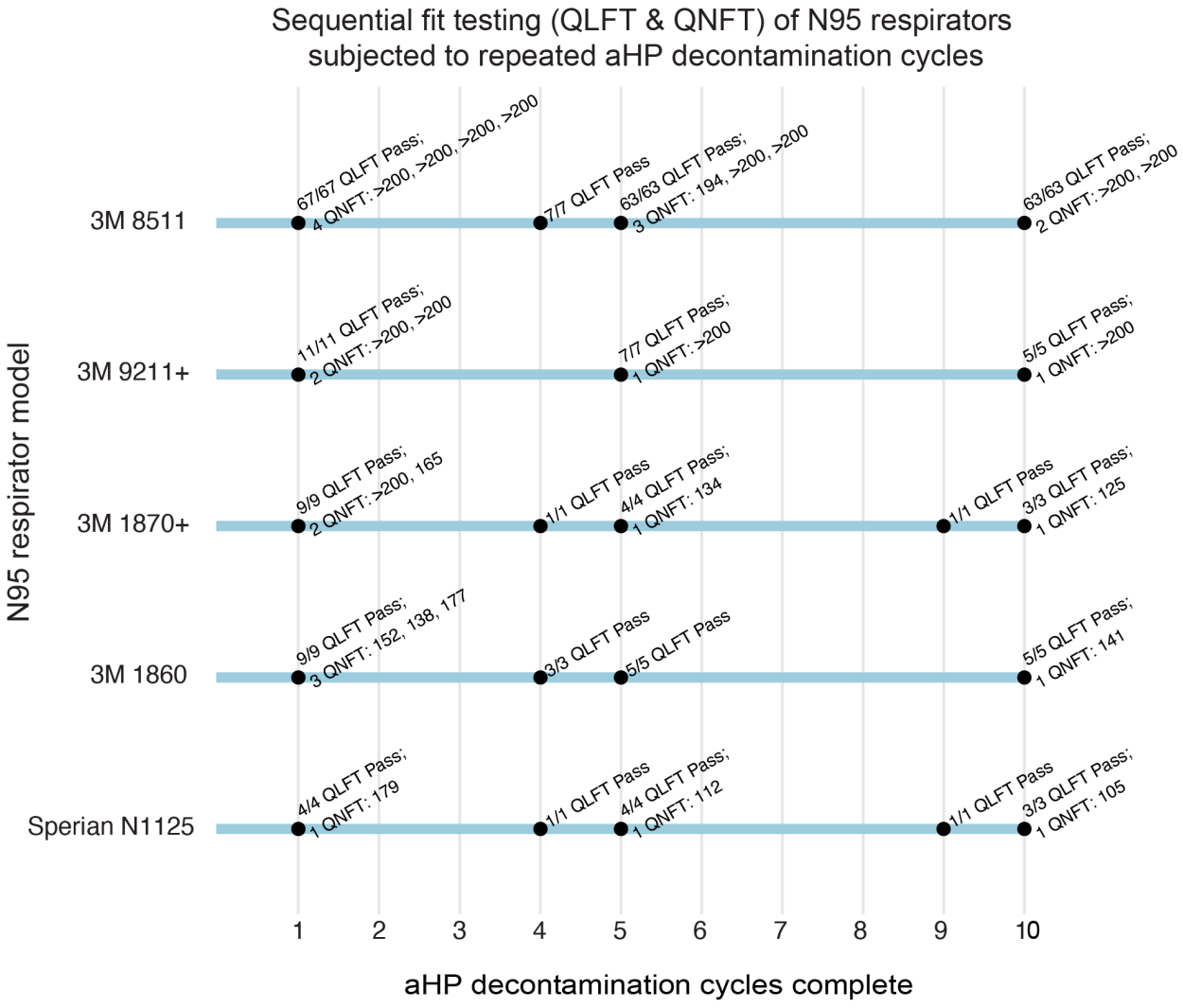

682

683 **Figure 1: Sequential fit testing (QLFT & QNFT) of N95 respirators subjected to repeated**
684 **aHP decontamination cycles.** Results demonstrate that all 3M model 8511 respirators
685 successfully pass QLFT and QNFT after 1, 5, and 10 cycles. In particular, 8 of 9 QNFT results
686 for the 3M model 8511 respirator surpassed a fit factor of 200, the maximum reportable by the
687 test method – providing qualitative, yet objective, evidence of the safety margin related to fit

688 integrity after 10 aHP decontamination cycles. All respirator models except Alpha Protech
689 (which had inconsistent fit-test results; see Methods for details) passed all QLFT and QNFT to
690 which they were subjected. Models Alpha ProTech (aHP cycle 1) and Kimberly Clark (aHP
691 cycle 2) were only included for a single cycle and are thus not shown here.

692

693 **Figure 2: Infectious titer of phi6 bacteriophage inoculated on N95 respirator**
694 **facepieces was eliminated after aerosolized H_2O_2 decontamination.**

695

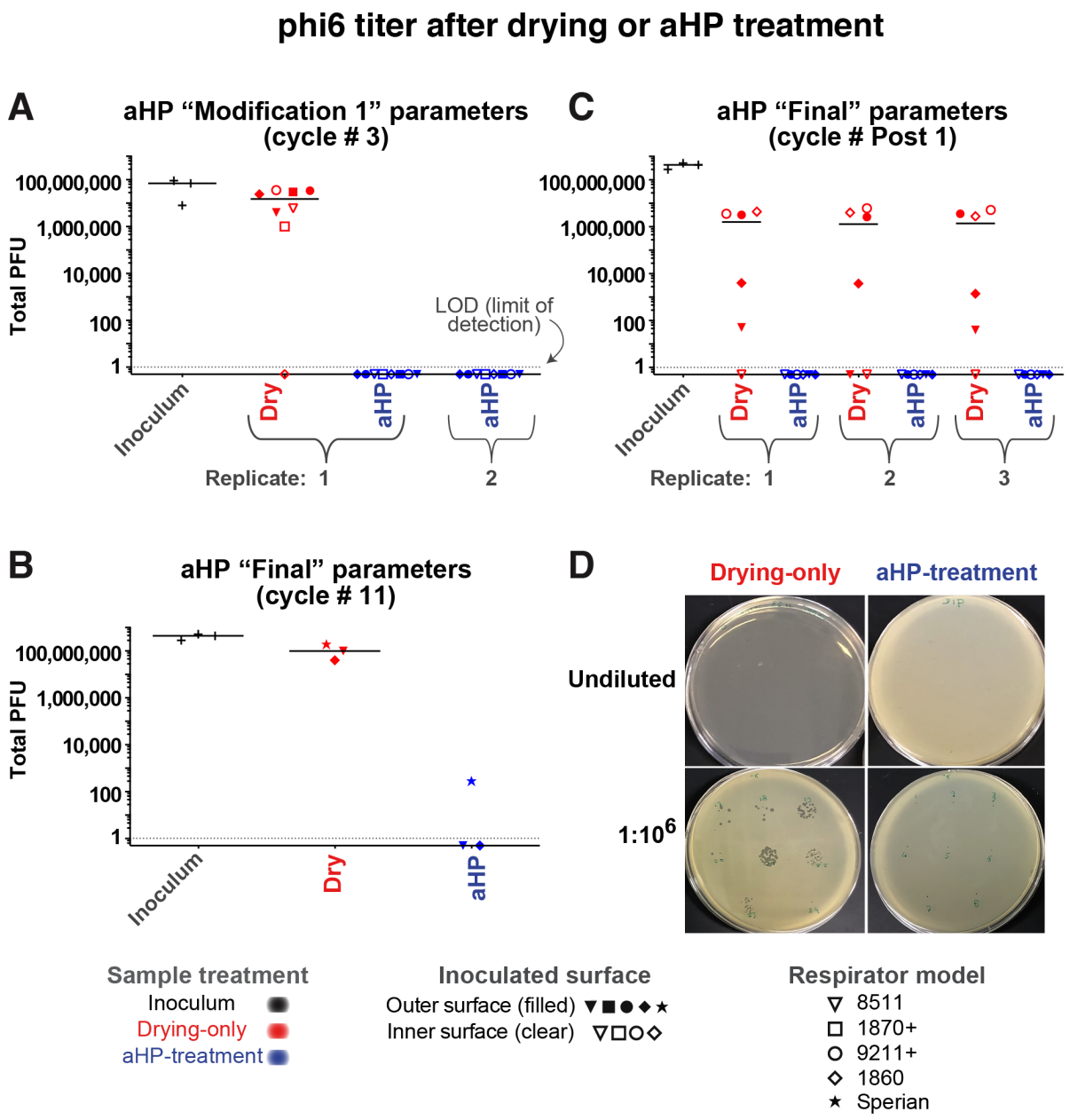

696

697 **Figure 2: Infectious titer of phi6 bacteriophage inoculated on N95 respirator facepieces was**
698 **eliminated after aerosolized H_2O_2 (aHP) decontamination.** (A-C) Data are plotted separately
699 for each aHP cycle in which viral testing was done (see Table 4). Multiple models of N95
700 respirator (see **Table 1**) were inoculated and either treated as "drying only" controls (red), or
701 subjected to aHP treatment (blue). The respirator surface and model are indicated by the symbol

shape and fill. The median of all points within a given aHP cycle and treatment is indicated by a solid horizontal line. The dashed horizontal line indicates the limit of detection (LOD) at 1 viral plaque-forming unit (PFU), in the resuspended but undiluted volume from the site of viral inoculation. (D) Image depicts Petri dish plating of bacterial lawns exposed to phi6 from drying-only (left side) or aHP-treated (right side) respirator inoculation sites. These were applied to the bacterial lawn either as an undiluted resuspension (top row) or $1{:}10^6$ dilution applied to focal points (bottom row). For phi6, the only positive plaque occurring after aHP treatment occurred on in a round of testing without replicate samples (aHP cycle 11), and thus could not be validated. For the purposes of illustrating the decontaminated sites where zero plaques were detected, these numbers were replaced with fractional values (0.5), to allow their visualization on this log-scale plot. See Supplementary Table 1 for all data values.

714 **Figure 3: Infectious titer of HSV-1 inoculated on N95 respirator facepieces was**
715 **reduced by drying and eliminated after aerosolized H_2O_2 decontamination.**

716

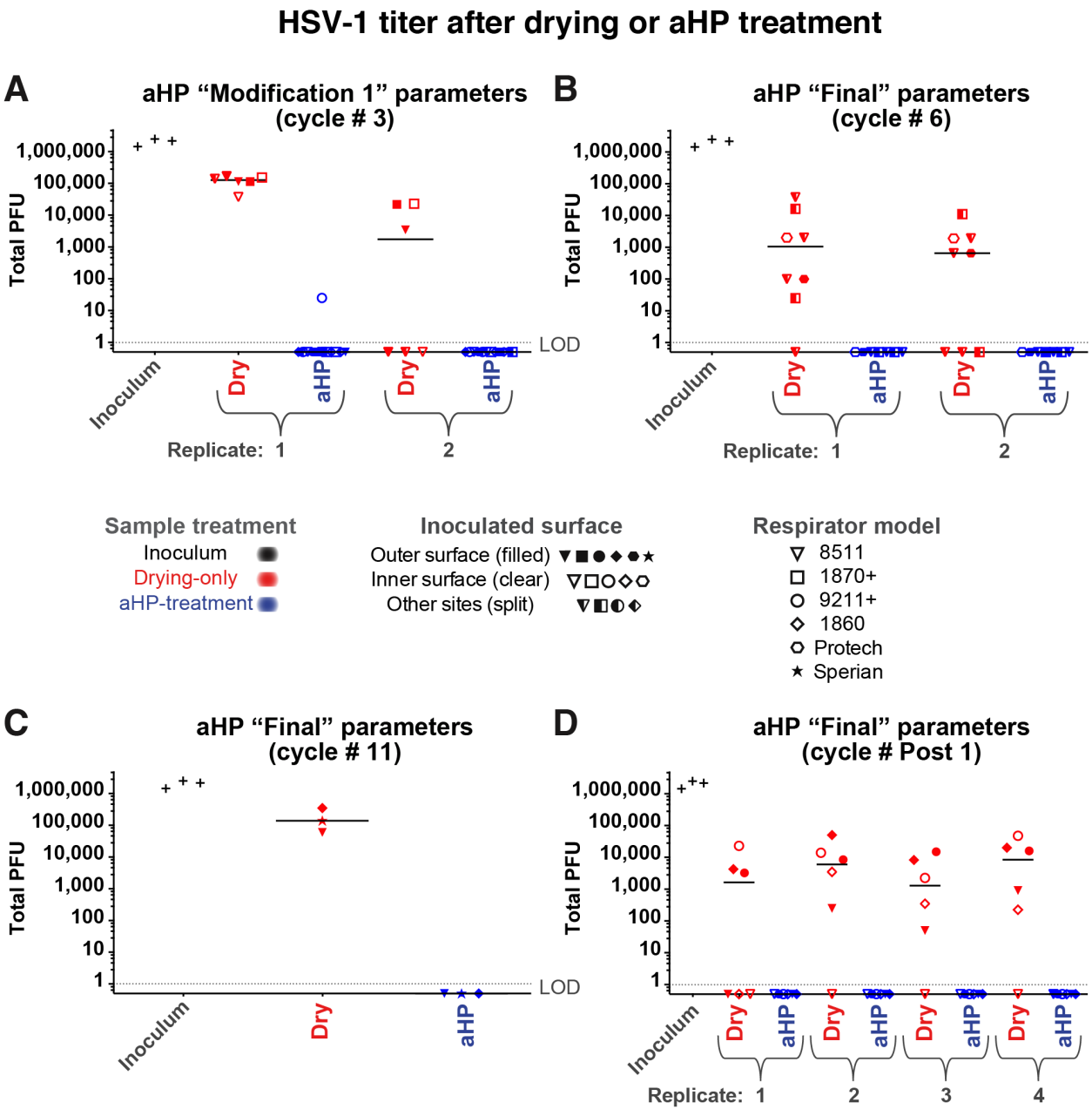

717

718 **Figure 3: Infectious titer of HSV-1 inoculated on N95 respirator facepieces was reduced by**
719 **drying and eliminated after aerosolized H_2O_2 (aHP) decontamination.** (A-D) Data are
720 plotted separately for each aHP cycle in which viral testing was done (see Table 4). For HSV-1,
721 the sole positive plaque after aHP treatment occurred in aHP cycle #3, when the "Modification
722 1" parameters were in use (Tables 3-4). This failure, in concert with a spore-based biological

723 indicator and 2 CVB3 plaques (Figure 4) motivated the addition of a "dwell time" in the final
724 aHP parameter. As in Figure 2, multiple models of N95 respirator (see Table 1) were inoculated
725 and either treated as "drying only" controls (red), or subjected to aHP treatment (blue). The
726 respirator surface and model are indicated by the symbol shape and fill. The median of all points
727 within a given aHP cycle and treatment is indicated by a solid horizontal line. The dashed
728 horizontal line indicates the limit of detection (LOD) at 1 viral plaque-forming unit (PFU), in the
729 resuspended but undiluted volume from the site of viral inoculation. For the purposes of
730 illustrating the decontaminated sites where zero plaques were detected, these numbers were
731 replaced with fractional values (0.5), to allow their visualization on this log-scale plot. Note that
732 the same HSV-1 starting inoculum values (titered in triplicate) are included on each plot, for
733 comparison to drying and aHP-treated values. See Supplementary Table 1 for all data values.

734

735 **Figure 4: Infectious titer of CVB3 inoculated on N95 respirator facepieces was**
736 **reduced by drying and eliminated after aerosolized H_2O_2 decontamination.**

737

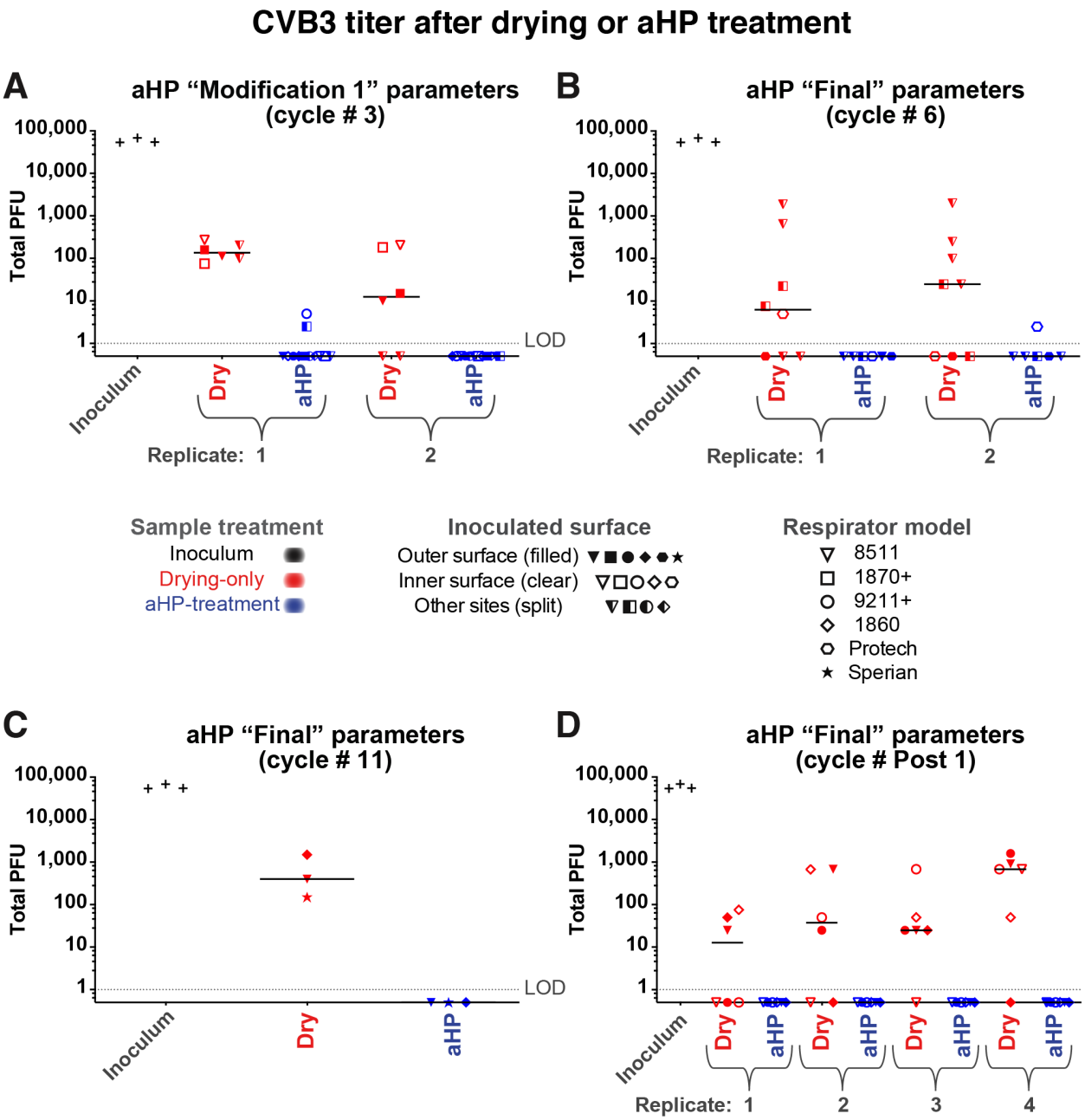

738

739 **Figure 4: Infectious titer of CVB3 inoculated on N95 respirator facepieces was reduced by**
740 **drying and eliminated after aerosolized H_2O_2 (aHP) decontamination.** (A-D) Data are
741 plotted separately for each aHP cycle in which viral testing was done (see Table 4). For CVB3,
742 two positive plaques after aHP treatment occurred in aHP cycle #3, when the "Modification 1"

743 parameters were in use (Tables 3-4). This failure, in concert with a spore-based biological
744 indicator and 1 HSV-1 plaques (Figure 4) motivated the addition of a "dwell time" in the final
745 aHP parameter. The only other positive CVB3 plaque after aHP treatment occurred in aHP cycle
746 6 (B), and no plaques were detected in the replicate or in parallel samples. As in Figure 2,
747 multiple models of N95 respirator (see Table 1) were inoculated and either treated as "drying
748 only" controls (red), or subjected to aHP treatment (blue). The respirator surface and model are
749 indicated by the symbol shape and fill. The median of all points within a given aHP cycle and
750 treatment is indicated by a solid horizontal line. The dashed horizontal line indicates the limit of
751 detection (LOD) at 1 viral plaque-forming unit (PFU), in the resuspended but undiluted volume
752 from the site of viral inoculation. For the purposes of illustrating the decontaminated sites where
753 zero plaques were detected, these numbers were replaced with fractional values (0.5), to allow
754 their visualization on this log-scale plot. Note that the same CVB3 starting inoculum values
755 (titered in triplicate) are included on each plot, for comparison to drying and aHP-treated values.
756 See Supplementary Table 1 for all data values.

757

758 **Figure 5: Infectious titer of SARS-CoV-2 inoculated on N95 respirator facepieces**
759 **was reduced by drying and eliminated after aerosolized H_2O_2 decontamination.**

760

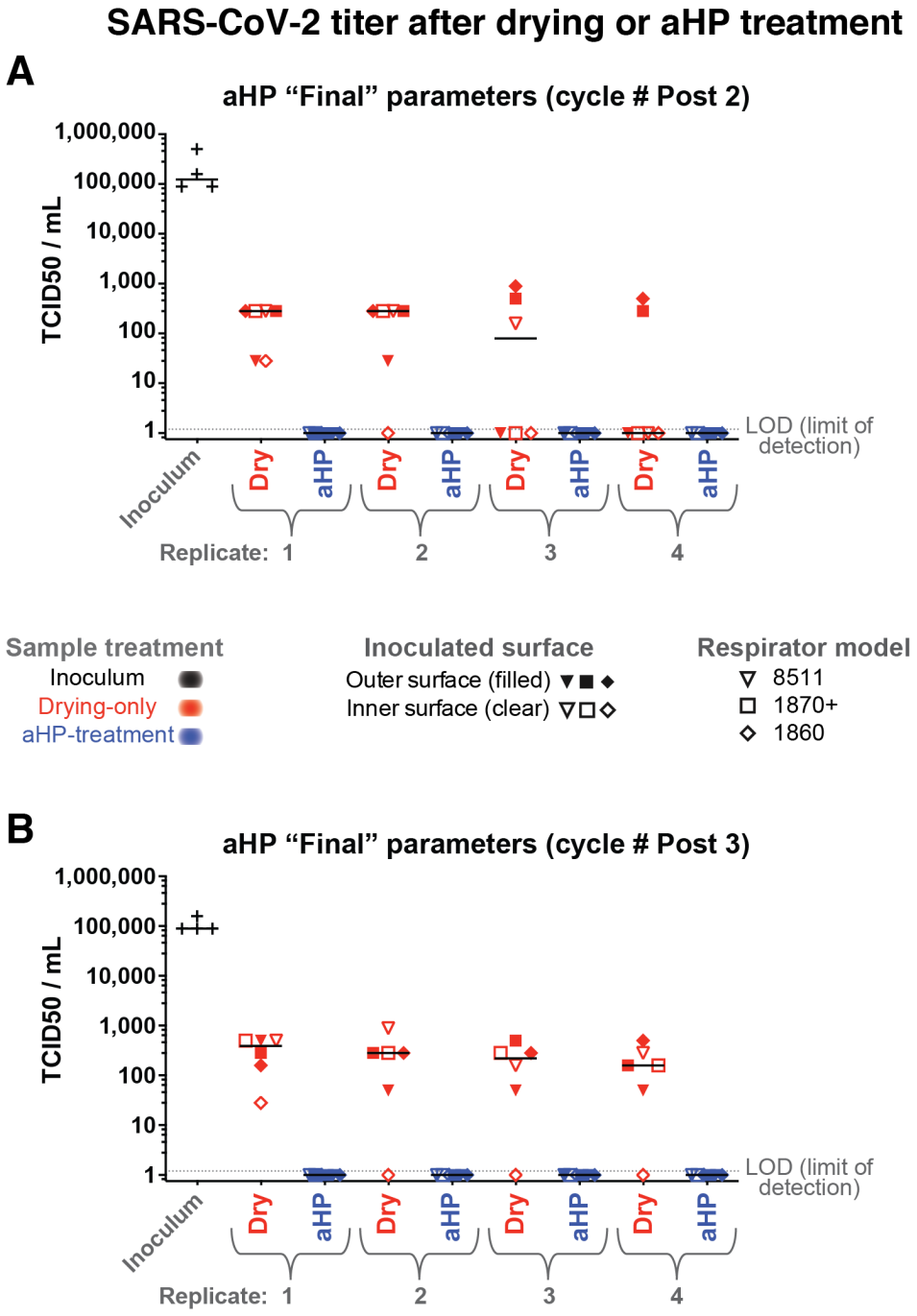

761

762 **Figure 4: Infectious titer of SARS-CoV-2 inoculated on N95 respirator facepieces was**
763 **reduced by drying and eliminated after aerosolized H_2O_2 (aHP) decontamination.** (A-B)
764 Data are plotted separately for each aHP cycle in which viral testing was done (see Table 4). For

765 SARS-CoV-2, no infectious virus was detected by TCID50 assay after aHP treatment. As in
766 Figure 2, multiple models of N95 respirator (see Table 1) were inoculated and either treated as
767 "drying only" controls (red), or subjected to aHP treatment (blue). The respirator surface and
768 model are indicated by the symbol shape and fill. The median of all points within a given aHP
769 cycle and treatment is indicated by a solid horizontal line. Viral titer was determined by tissue
770 culture infectious dose 50 (TCID50) assay in 96-well plates, with a limit of detection (LOD) of
771 1.2 (see Methods for details). For the purposes of illustrating the decontaminated samples where
772 no virus was detected, these numbers were plotted as a value of 1. See Supplementary Table 1
773 for all data values.

774

775 # References

776 1. Rutala WA, Weber DJ, Healthcare Infection Control Practices Advisory Committee
777 (HICPAC). 2008. Guideline for Disinfection and Sterilization in Healthcare Facilities,
778 2008. Cent Dis Control CDC 163.

779 2. Centers for Disease Control and Prevention, National Center for Emerging and Zoonotic
780 Infectious Diseases (NCEZID), Division of Healthcare Quality Promotion (DHQP). 2008.
781 Guideline for Disinfection and Sterilization in Healthcare Facilities. Sterilizing Pract
782 Disinfect Steriliz Guidel Guidel Libr Infect Control CDC.

783 3. 3M Personal Safety Division. 2020. Disinfection of Filtering Facepiece Respirators. 3M
784 Tech Bull 4.

785 4. Battelle Memorial Institute. 2016. Final Report for the Bioquell Hydrogen Peroxide Vapor
786 (HPV) Decontamination for Reuse of N95 Respirators. Prep Contract – Study Number
787 3245 US Food Drug Adm 46.

788 5. Liao L, Xiao W, Zhao M, Yu X, Wang H, Wang Q, Chu S, Cui Y. 2020. Can N95
789 Respirators Be Reused after Disinfection? How Many Times? ACS Nano 14:6348–6356.

790 6. Schwartz A, Stiegel M, Greeson N, Vogel A, Thomann W, Brown M, Sempowski GD,
791 Alderman TS, Condreay JP, Burch J, Wolfe C, Smith B, Lewis S. 2020. Decontamination
792 and Reuse of N95 Respirators with Hydrogen Peroxide Vapor to Address Worldwide
793 Personal Protective Equipment Shortages During the SARS-CoV-2 (COVID-19) Pandemic.
794 Appl Biosaf 25:67–70.

795 7. Goyal SM, Chander Y, Yezli S, Otter JA. 2014. Evaluating the virucidal efficacy of
796 hydrogen peroxide vapour. J Hosp Infect 86:255–259.

797 8. Tuladhar E, Terpstra P, Koopmans M, Duizer E. 2012. Virucidal efficacy of hydrogen
798 peroxide vapour disinfection. J Hosp Infect 80:110–115.

799 9. Holmdahl T, Odenholt I, Riesbeck K, Medstrand P, Widell A. 2019. Hydrogen peroxide
800 vapour treatment inactivates norovirus but has limited effect on post-treatment viral RNA
801 levels. Infect Dis 51:197–205.

802 10. Hultman C, Hill A, McDonnell G. 2006. The physical chemistry of decontamination with
803 gaseous hydrogen peroxide. Pharm Eng 27:22–32.

804 11. Otter JA, Yezli S. 2011. A call for clarity when discussing hydrogen peroxide vapour and
805 aerosol systems. J Hosp Infect 77:83–84.

806 12. Boyce JM. 2009. New Approaches to Decontamination of Rooms After Patients Are
807 Discharged. Infect Control Hosp Epidemiol 30:515–517.

808 13. Fu TY, Gent P, Kumar V. 2012. Efficacy, efficiency and safety aspects of hydrogen peroxide
809 vapour and aerosolized hydrogen peroxide room disinfection systems. J Hosp Infect
810 80:199–205.

811 14. Holmdahl T, Lanbeck P, Wullt M, Walder MH. 2011. A Head-to-Head Comparison of
812 Hydrogen Peroxide Vapor and Aerosol Room Decontamination Systems. Infect Control
813 Hosp Epidemiol 32:831–836.

814 15. Freyssenet C, Karlen S. 2019. Plasma-Activated Aerosolized Hydrogen Peroxide (aHP) in
815 Surface Inactivation Procedures. Appl Biosaf 24:10–19.

816 16. Best EL, Parnell P, Thirkell G, Verity P, Copland M, Else P, Denton M, Hobson RP, Wilcox
817 MH. 2014. Effectiveness of deep cleaning followed by hydrogen peroxide decontamination
818 during high Clostridium difficile infection incidence. J Hosp Infect 87:25–33.

819 17. Barbut F, Menuet D, Verachten M, Girou E. 2009. Comparison of the Efficacy of a
820 Hydrogen Peroxide Dry-Mist Disinfection System and Sodium Hypochlorite Solution for
821 Eradication of *Clostridium difficile* Spores. Infect Control Hosp Epidemiol 30:507–514.

822 18. Shapey S, Machin K, Levi K, Boswell TC. 2008. Activity of a dry mist hydrogen peroxide
823 system against environmental Clostridium difficile contamination in elderly care wards. J
824 Hosp Infect 70:136–141.

825 19. Bartels MD, Kristoffersen K, Slotsbjerg T, Rohde SM, Lundgren B, Westh H. 2008.
826 Environmental meticillin-resistant Staphylococcus aureus (MRSA) disinfection using dry-
827 mist-generated hydrogen peroxide. J Hosp Infect 70:35–41.

828 20. Andersen BM, Syversen G, Thoresen H, Rasch M, Hochlin K, Seljordslia B, Snevold I, Berg
829 E. 2010. Failure of dry mist of hydrogen peroxide 5% to kill Mycobacterium tuberculosis. J
830 Hosp Infect 76:80–83.

831 21. Beswick AJ, Farrant J, Makison C, Gawn J, Frost G, Crook B, Pride J. 2011. Comparison of
832 Multiple Systems for Laboratory Whole Room Fumigation. Appl Biosaf 16:139–157.

833 22. The National Institute for Occupational Safety and Health (NIOSH). 2020. Recommended
834 Guidance for Extended Use and Limited Reuse of N95 Filtering Facepiece Respirators in
835 Healthcare Settings. NIOSH Workplace Saf Health Top.

836 23. Hinton, Chief Scientist, Food and Drug Administration D. 2020. FDA Letter - Emergency
837 Use Authorization (EUA) for the Battelle Critical Care Decontamination System (CCDS).

838 24. Schwartz A, Stiegel M, Greeson N, Vogel A, Thomann W, Brown M, Sempowski GD,
839 Alderman TS, Condreay JP, Burch J, Wolfe C, Smith B, Lewis S. 2020. Decontamination
840 and Reuse of N95 Respirators with Hydrogen Peroxide Vapor to Address Worldwide
841 Personal Protective Equipment Shortages During the SARS-CoV-2 (COVID-19) Pandemic.
842 Appl Biosaf 153567602091993.

843 25. Kenney P, Chan BK, Kortright K, Cintron M, Havill N, Russi M, Epright J, Lee L, Balcezak
844 T, Martinello R. 2020. Hydrogen Peroxide Vapor sterilization of N95 respirators for reuse.
845 medRxiv preprint.

846 26. Kumar A, Kasloff SB, Leung A, Cutts T, Strong JE, Hills K, Gu FX, Chen P, Vazquez-
847 Grande G, Rush B, Lother S, Malo K, Zarychanski R, Krishnan J. 2020. Decontamination
848 of N95 masks for re-use employing 7 widely available sterilization methods. PLOS ONE
849 15:e0243965.

850 27. Levine C, Grady C, Block T, Hurley H, Russo R, Peixoto B, Frees A, Ruiz A, Alland D.
851 2021. Use, re-use or discard? Quantitatively defined variance in the functional integrity of

852 N95 respirators following vaporized hydrogen peroxide decontamination during the
853 COVID-19 pandemic. J Hosp Infect 107:50–56.

854 28. Fischer RJ, Morris DH, van Doremalen N, Sarchette S, Matson MJ, Bushmaker T, Yinda
855 CK, Seifert SN, Gamble A, Williamson BN, Judson SD, de Wit E, Lloyd-Smith JO,
856 Munster VJ. 2020. Effectiveness of N95 Respirator Decontamination and Reuse against
857 SARS-CoV-2 Virus. Emerg Infect Dis 26:2253–2255.

858 29. Oral E, Wannomae KK, Connolly RL, Gardecki JA, Leung HM, Muratoglu OK, Durkin J,
859 Jones R, Collins C, Gjore J, Budzilowicz A, Jaber T. 2020. Vaporized H_2O_2
860 decontamination against surrogate viruses for the reuse of N95 respirators in the COVID-19
861 emergency. preprint, Occupational and Environmental Health.

862 30. Grillet AM, Nemer MB, Storch S, Sanchez AL, Piekos ES, Leonard J, Hurwitz I, Perkins DJ.
863 2020. COVID-19 global pandemic planning: Performance and electret charge of N95
864 respirators after recommended decontamination methods. Exp Biol Med
865 153537022097638.

866 31. Rockey N, Arts PJ, Li L, Harrison KR, Langenfeld K, Fitzsimmons WJ, Lauring AS, Love
867 NG, Kaye KS, Raskin L, Roberts WW, Hegarty B, Wigginton KR. 2020. Humidity and
868 Deposition Solution Play a Critical Role in Virus Inactivation by Heat Treatment of N95
869 Respirators. mSphere 5.

870 32. Occupational Safety and Health Administration (OSHA), United States Department of
871 Labor. Limits for Air Contaminants. 19101000 TABLE Z-1 - TABLE Z-1.

872 33. American Conference of Governmental Industrial Hygienists (ACGIH). 2019. Hydrogen
873 Peroxide: Threshold Limit Values (TLV) Chemical Substances, 7th ed. Cincinnati, OH.

874 34. Steris Healthcare. Biological Indicators for Sterilization | STERIS.

875 35. Advanced Chemical Sensors. AIHA-LAP ID No. 102047. Longwood, Florida.

876 36. SGS Galson Laboratories. AIHA-LAP ID No. 100324. E. Syracuse, New York 13057.

877 37. Occupational Safety and Health Administration (OSHA), United States Department of
878 Labor. Fit Testing Procedures (Mandatory). Respir Prot Stand 29 CFR 1910134 F – Fit Test
879 Append Subpart B3 – Qual Fit-Test QLFT Protoc Saccharine Solut Aerosol Protoc Subpart
880 C3 – Quant Fit-Test QNFT Protoc Ambient Aerosol Condens Nucl Count CNC Quant Fit
881 Test Protoc. https://www.osha.gov/laws-
882 regs/regulations/standardnumber/1910/1910.134AppA.

883 38. Operation and Service Manual. 2015. Portacount Pro 8030 and Portacount Pro+ 8038
884 Respirator Fit TestersRev. P. T.S.I., Inc., Shoreview, MN.

885 39. National Institute for Occupational Safety and Health. 2019. Determination of Particulate
886 Filter Efficiency Level for N95 Series Filters Against Solid Particulates for Non-Powered,
887 Air-Purifying Respirators Standard Testing Procedure (STP), p. 9. *In* TEB-APR-STEP-
888 0059Revision 3.2. https://www.cdc.gov/niosh/npptl/stps/apresp.html.

889 40. Hockett KL, Baltrus DA. 2017. Use of the Soft-agar Overlay Technique to Screen for
890 Bacterially Produced Inhibitory Compounds. J Vis Exp https://doi.org/10.3791/55064.

891 41. Reed LJ, Muench H. 1938. A simple method of estimating fifty per cent endpoints. Am J
892 Epidemiol 27:493–497.

893 42. 3M Personal Safety Division. 3M^{TM} Aura^{TM} Health Care Particulate Respirator and Surgical
894 Mask 1870+, N95.

895 43. Centers for Disease Control and Prevention (CDC). 2020. Implementing Filtering Facepiece
896 Respirator (FFR) Reuse, Including Reuse after Decontamination, When There Are Known
897 Shortages of N95 Respirators. Coronavirus Dis 2019 COVID-19.

898 44. van Doremalen N, Bushmaker T, Morris DH, Holbrook MG, Gamble A, Williamson BN,
899 Tamin A, Harcourt JL, Thornburg NJ, Gerber SI, Lloyd-Smith JO, de Wit E, Munster VJ.
900 2020. Aerosol and Surface Stability of SARS-CoV-2 as Compared with SARS-CoV-1. N
901 Engl J Med https://doi.org/10.1056/NEJMc2004973.

902 45. Sizun J, Yu MWN, Talbot PJ. 2000. Survival of human coronaviruses 229E and OC43 in
903 suspension and after drying onsurfaces: a possible source ofhospital-acquired infections. J
904 Hosp Infect 46:55–60.

905 46. Duan S-M, Zhao X-S, Wen R-F, Huang J-J, Pi G-H, Zhang S-X, Han J, Bi S-L, Ruan L,
906 Dong X-P, SARS Research Team. 2003. Stability of SARS coronavirus in human
907 specimens and environment and its sensitivity to heating and UV irradiation. Biomed
908 Environ Sci BES 16:246–255.

909 47. Rabenau HF, Cinatl J, Morgenstern B, Bauer G, Preiser W, Doerr HW. 2005. Stability and
910 inactivation of SARS coronavirus. Med Microbiol Immunol (Berl) 194:1–6.

911 48. Geller C, Varbanov M, Duval R. 2012. Human Coronaviruses: Insights into Environmental
912 Resistance and Its Influence on the Development of New Antiseptic Strategies. Viruses
913 4:3044–3068.

914 49. Firquet S, Beaujard S, Lobert P-E, Sané F, Caloone D, Izard D, Hober D. 2015. Survival of
915 Enveloped and Non-Enveloped Viruses on Inanimate Surfaces. Microbes Environ 30:140–
916 144.

917 50. Kampf G, Todt D, Pfaender S, Steinmann E. 2020. Persistence of coronaviruses on
918 inanimate surfaces and their inactivation with biocidal agents. J Hosp Infect 104:246–251.

919 51. Vasickova P, Pavlik I, Verani M, Carducci A. 2010. Issues Concerning Survival of Viruses
920 on Surfaces. Food Environ Virol 2:24–34.

921
922
923

Supplementary Figures

Supplementary Figure 1: Respirators positioned on rack

Respirator staging (partial loading) on metal rack with binder clips and rack centrally positioned in the Prep Room.

931

932

933 **Supplementary Figure 2: Curis® unit.**

934 Curis® decontamination unit with adjustable aHP dispersal nozzle and programmable inputs.

935

Supplementary Figure 3: Prep Room door seal

Door sealed with polyethylene sheeting and non-porous adhesive tape to prevent migration of H_2O_2 outside of the Prep Room.

Supplementary Figure 4: BIs positioned within nested N95 respirators

In order to test the ability of aHP under these cycle parameters to penetrate respirator material, biological indicators (BI's) (*Geobacillius stearothermophilis*) were nested between two molded respirators (3M 1860) and taped together, or BIs were enclosed within a flat-fold type respirator (3M Aura 9211+; not pictured). All BIs positioned in this manner were rendered inactivated after aHP treatment.

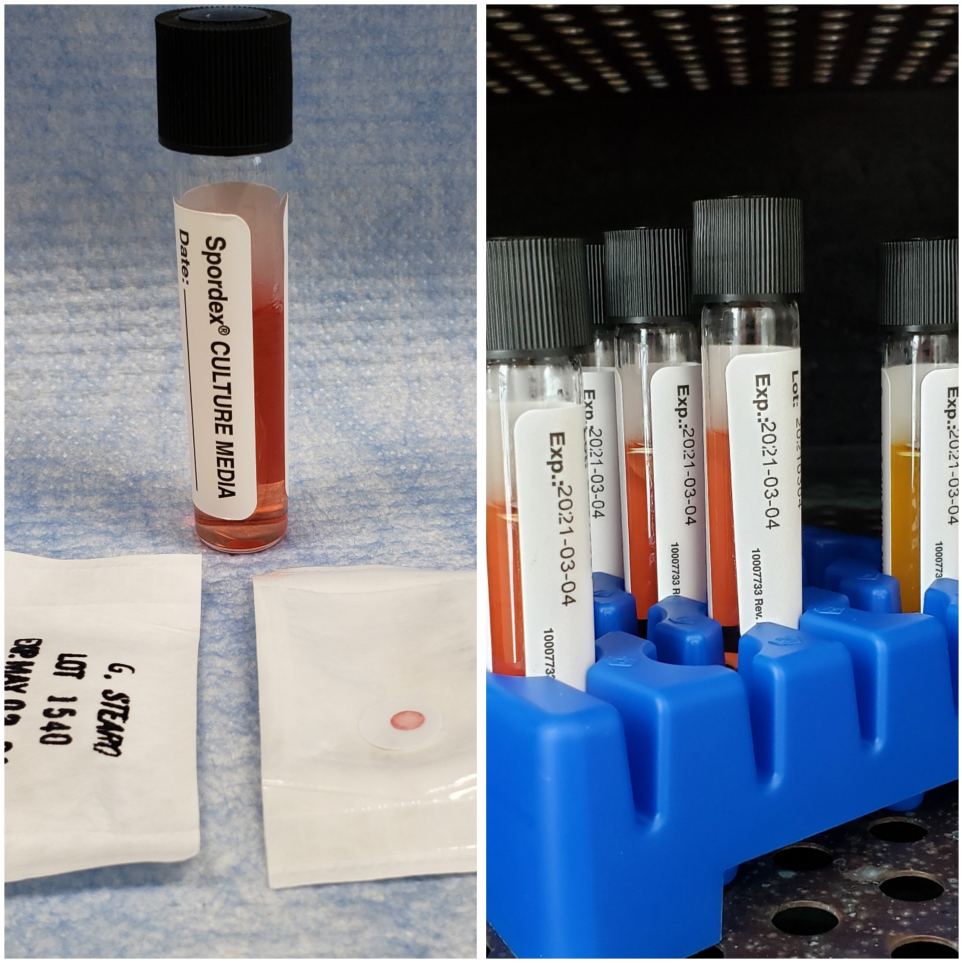

Supplementary Figure 5: Cultures of spore-based biological indicators

Biological indicator spore discs are transferred from Tyvek/glassine envelopes to culture media and incubated for at 55°C for at least 7 days post decontamination cycle. Media color change to yellow indicates bacterial growth, as seen in the positive control tube on the far right.

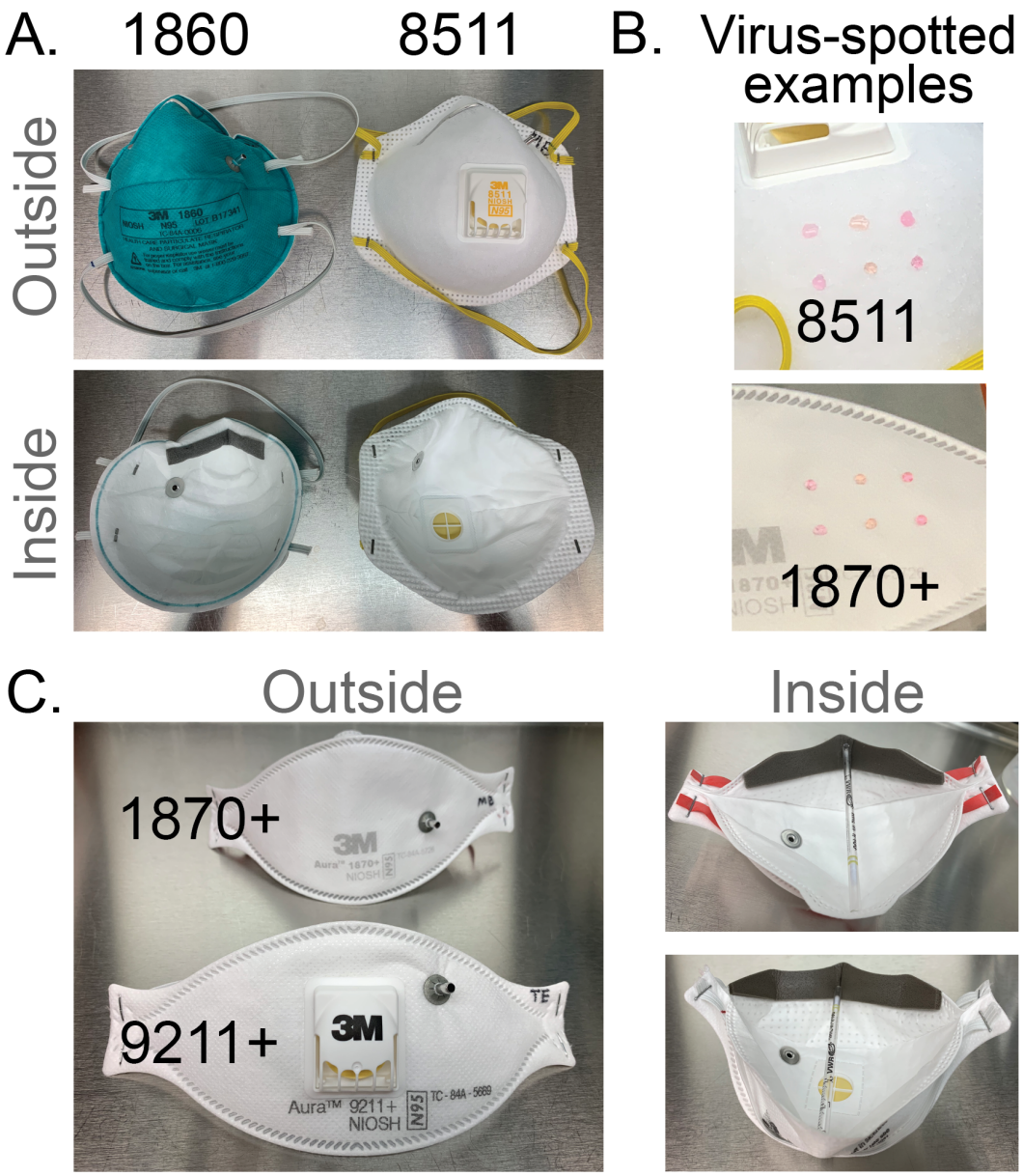

Supplementary Figure 6: Respirator facepiece models & characteristics

(A) 3M models 1860 and 8511 (left) have a molded facepiece, with 8511 including an exhalation valve. **(B)** Virus-inoculation via droplets spotted onto the respirator fabric are shown for two examples. **(C)** 3M models 1870+ and 9211+ share a common folded fabric model, with a high fluid resistance of the fabric. 3M 9211+ includes an exhalation valve. Several of the facepieces (1860, 1870+, 9211+) display the metal grommet from insertion of the probe used for quantitative fit testing (QNFT). The inner face of each respirator is shown, which for the models shown in **(C)** required a prop to hold them open.

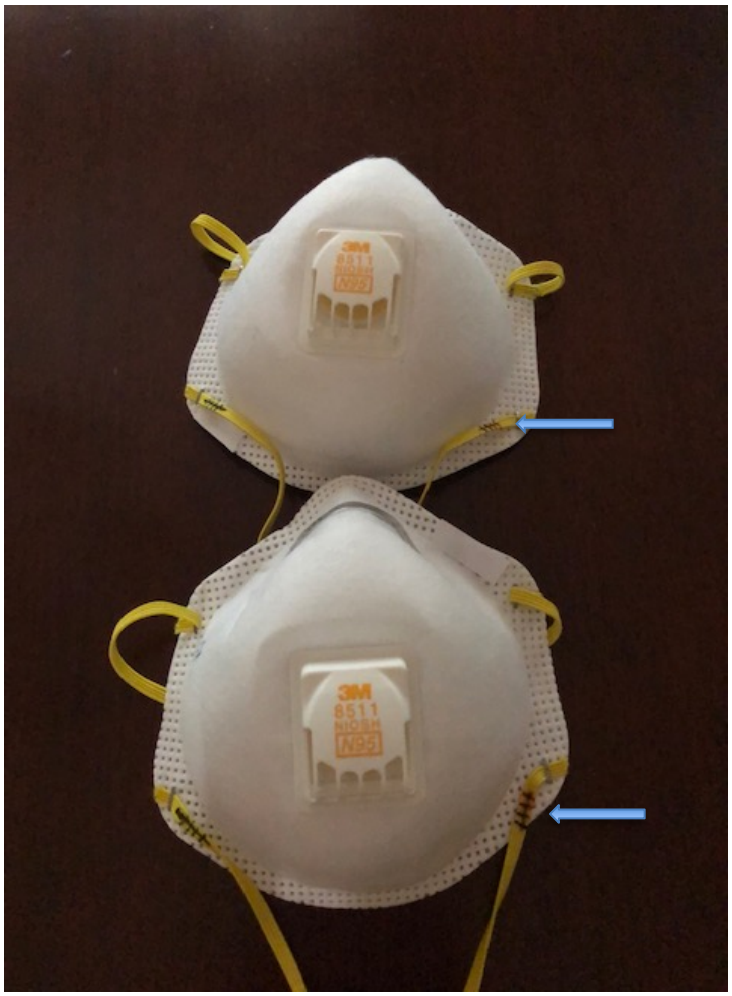

Supplementary Figure 7: Respirator aHP cycle markings

Indelible ink pen hash marks (noted at lower respirator straps) placed to notate completed aHP cycle, at time of cycle completion, or collection/transport for subsequent fit-testing or virus inactivation testing.

975

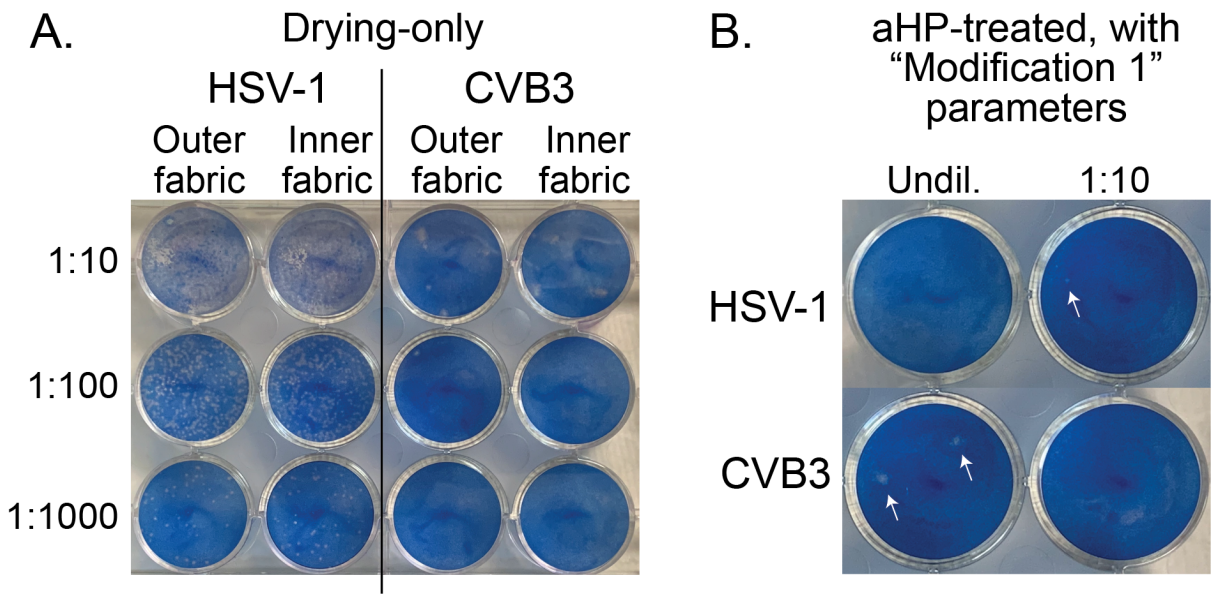

976

977 **Supplementary Figure 8: Viral titration demonstrates inactivation and loss of**
978 **infectious units due to drying and aerosolized H_2O_2 (aHP) decontamination**

979 Shown here are representative examples of serial dilutions (titration) of HSV-1 or CVB3 that
980 were spotted onto 3M 9211+ respirators, and then resuspended and plated onto monolayers of
981 Vero detector cells. Viral plaques, which are visible as clear foci of infection (plaque-forming
982 units, or PFU) on the background of methylene blue-stained cells, were visualized at 72 hours
983 post infection. The plate shown in **(A)** illustrates serial dilution of a high concentration of HSV-1
984 after drying (10^5 PFU; see plot in Figure 3A), and a lower concentration of CVB3 after drying
985 (10^2 PFU; see plot in Figure 4A). The plate shown in **(B)** is from an aHP cycle run with
986 "Modification 1" parameters, when no dwell time was used (aHP cycle 3; see Tables 3-4) and
987 commercial spore-based biological indicators indicated a failure of decontamination. Even on
988 this partial aHP decontamination, only three wells (of which two are shown above) had any viral
989 plaques (indicated by arrowheads; these equate to 25 PFU of HSV-1, and 5 PFU of CVB3; see
990 plots in Figure 3A and 4A).

991

992 # Supplementary Table (separate Excel file)

993 ## Supplementary Table 1 (Excel): aHP Viral Testing Values

994 Data underlying Figures 2-4, and Table 4. These include the number of plaque-forming units
995 (PFU) for phi6, HSV-1, and CVB3, as well as TCID50(log10)/mL values for SARS-CoV-2. As
996 noted in Figures 2-4, for samples where no virus was detected, these numbers were replaced with
997 non-zero values to allow their visualization on the log-scale plots in Figures 2-4. HSV-1, CVB3,
998 and phi6 "no virus detected" values were set to 0.5 (less than 1 plaque detected), and SARS-
999 CoV-2 values were set to 1 (less than the limit of detection of 1.2 TCID50(log10)/mL).